AD_____

Award Number: DAMD17-99-1-9142

TITLE: Mechanisms of Growth Factor Attenuation of Cell Death in
Chemotherapy Treated Breast Cancer Cells

PRINCIPAL INVESTIGATOR: Carla Van Den Berg, Ph.D.

CONTRACTING ORGANIZATION: University of Colorado Health Sciences
Center
Denver, Colorado 80262

REPORT DATE: August 2003

TYPE OF REPORT: Annual Summary

PREPARED FOR: U.S. Army Medical Research and Materiel Command
Fort Detrick, Maryland 21702-5012

DISTRIBUTION STATEMENT: Approved for Public Release;
Distribution Unlimited

The views, opinions and/or findings contained in this report are
those of the author(s) and should not be construed as an official
Department of the Army position, policy or decision unless so
designated by other documentation.

20040706 129

REPORT DOCUMENTATION PAGE	Form Approved OMB No. 074-0188

Public reporting burden for this collection of information is estimated to average 1 hour per response, including the time for reviewing instructions, searching existing data sources, gathering and maintaining the data needed, and completing and reviewing this collection of information. Send comments regarding this burden estimate or any other aspect of this collection of information, including suggestions for reducing this burden to Washington Headquarters Services, Directorate for Information Operations and Reports, 1215 Jefferson Davis Highway, Suite 1204, Arlington, VA 22202-4302, and to the Office of Management and Budget, Paperwork Reduction Project (0704-0188), Washington, DC 20503

1. AGENCY USE ONLY (Leave blank)	2. REPORT DATE August 2003	3. REPORT TYPE AND DATES COVERED Annual Summary (1 Aug 99 – 31 Jul 03)

4. TITLE AND SUBTITLE Mechanisms of Growth Factor Attenuation of Cell Death in Chemotherapy Treated Breast Cancer Cells	5. FUNDING NUMBERS DAMD17-99-1-9142

6. AUTHOR(S)
Carla Van Den Berg, Ph.D.

7. PERFORMING ORGANIZATION NAME(S) AND ADDRESS(ES) University of Colorado Health Sciences Center Denver, Colorado 80262 E-Mail: carla.vandenberg@uchsc.edu	8. PERFORMING ORGANIZATION REPORT NUMBER

9. SPONSORING / MONITORING AGENCY NAME(S) AND ADDRESS(ES) U.S. Army Medical Research and Materiel Command Fort Detrick, Maryland 21702-5012	10. SPONSORING / MONITORING AGENCY REPORT NUMBER

11. SUPPLEMENTARY NOTES

12a. DISTRIBUTION / AVAILABILITY STATEMENT Approved for Public Release; Distribution Unlimited	12b. DISTRIBUTION CODE

13. ABSTRACT (Maximum 200 Words)
The purpose of this research project was study the mechanisms for insulin-like growth factor-I (IGF-I) mediated survival responses in breast cancer cells treated with chemotherapy or radiation. To this end, we have focused on the survival kinase, Akt and also the kinase which conveys cell death messages induced by chemotherapy or radiation treatment, JNK (c-Jun N-terminal kinase). Interestingly, IGF-I treatment of breast cancer cells induces the activity of both kinases Akt and JNK. Our recent work with Akt confirm that its activity protects cells form chemotherapy. The MCF-7 breast cancer cell line that we use for our studies is protected from IGF-I activation of Akt but not through pathways that have been described thus far. In fact, these cells are resistant to the cell death pathway that is typically activated with chemotherapy and radiation treatment. Therefore, we are currently studying new mechanisms for Akt mediated cell survival. Our work to identify how JNK conveys cell death signals in response to UV or chemotherapy treatment indicates that JNK can also down-regulates growth factor mediated signaling. Inhibition of JNK, in the absence of chemotherapy or radiation, also causes cell cycle arrest and inhibits breast cancer cell proliferation.

14. SUBJECT TERMS IGF-I, chemotherapy, signal transduction, PI 3-kinase, JNK	15. NUMBER OF PAGES 31
	16. PRICE CODE

17. SECURITY CLASSIFICATION OF REPORT Unclassified	18. SECURITY CLASSIFICATION OF THIS PAGE Unclassified	19. SECURITY CLASSIFICATION OF ABSTRACT Unclassified	20. LIMITATION OF ABSTRACT Unlimited

NSN 7540-01-280-5500

Standard Form 298 (Rev. 2-89)
Prescribed by ANSI Std. Z39-18
298-102

Table of Contents

Introduction

IGF-I receptor (IGF-IR) overexpression is a frequent aberration in found in breast tumors. IGF-IR activation may serve its greatest purpose in cancer cells by activating intracellular PI 3-kinase and its downstream target Akt to convey proliferation and survival of breast cancer cells. In breast cancer cell lines, treatment with IGF-I results in IGF-IR activation and tyrosine phosphorylation of the IRS-1 docking protein. The p85 subunit of PI 3-kinase then binds to IRS-1 to activate downstream kinases such as Akt and p70^{S6} kinase. IGF-IR is an important target for development of new breast cancer interventions since its expression has been observed in 87% of breast cancer specimens. Breast cancer cells expressing IGF-IR undergo a robust proliferative response when exposed to the receptor's ligands. A great amount of research has focused on the effect of growth factor activation of Akt on breast cancer cell survival, with the belief that Akt must convey the majority of PI 3-kinase effects. My lab has studied the survival responses induced by IGF-I treatment of breast cancer cells and how these responses may be altered by cellular stress, including chemotherapy and radiation treatment induction of the p53 tumor suppressor protein or JNK (c-Jun N-terminal kinase).

Body

Research accomplishments: In the past four years our efforts to identify the mechanisms of IGF-I pro-survival responses have been separated into two separate projects. Both of these projects stem from the Career Development Award. The first is to understand the mechanism(s) and/or effects of IGF-I activated JNK in breast cancer cells. We are also studying if the outcome of IGF-I activated JNK is p53 dependent. The second project is to understand how IGF-I activated Akt inhibits the apoptosis cascade of proteins. We initially anticipated that Akt would inhibit caspase 9 in a p53-dependent fashion. Our current results indicate otherwise. For purposes of this progress report, our findings will be presented as outlined in the initial Statement of Work of the application.

Task 1 is to describe IGF-IR cytoprotective effects through PI 3-kinase.

In previous progress reports we have demonstrated IGF-I's survival effects through activation of PI 3-kinase and Akt. Overexpression of a constitutively active form of Akt further supports our findings of Akt's survival properties. Thus, two years ago we were awarded an RO1 grant to study the effects of IGF-I activation of p53 mediated apoptosis. Caspases are family of proteases that become cleaved when activated by cellular stress. Upstream caspases then cleave downstream caspases. Ultimately, the activity of the caspases results in the morphological changes associated with apoptosis (programmed cell death). We anticipated that Akt would inhibit p53-mediated apoptosis by phosphorylation of caspase –9 and subsequent inhibition of its cleavage; caspase-9 is a downstream target of p53. Our recent data suggest that for some forms of DNA damage, Akt is working independently of caspase-9 in the MCF-7 breast cancer cells (Figure 1) (1). Our data show instead that Akt inhibits caspase-8 cleavage, a caspase which is typically activated in response to cytokine binding to death receptors like TNF-α or TRAIL (Figures 2 and 3). This work has recently been published in the *Journal of Biological Chemistry* (2). Our most recent unpublished studies show that IGF-I mediates its protective response through mTOR, another Akt target traditionally known for its role in protein translation. However in our model, protein translation is not required for this protective effect on cells. This suggests that mTOR is mediating this survival response in a post-translational fashion.
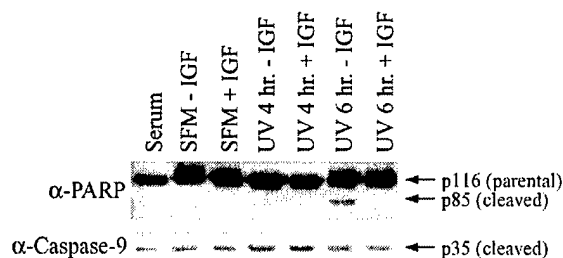

Figure 1. UV induced apoptosis and IGF-I mediated survival effects are caspase-9 independent. MCF-7 cells were plated and serum starved as described in Experimental Procedures. The following day cells were treated with UV irradiation (10 J/M^2) with or without IGF-I co-treatment (50 ng/ml). Six hours after treatment, cells were harvested and lysates subjected to Western blot analyses for PARP and pro-caspase-9 cleavage.
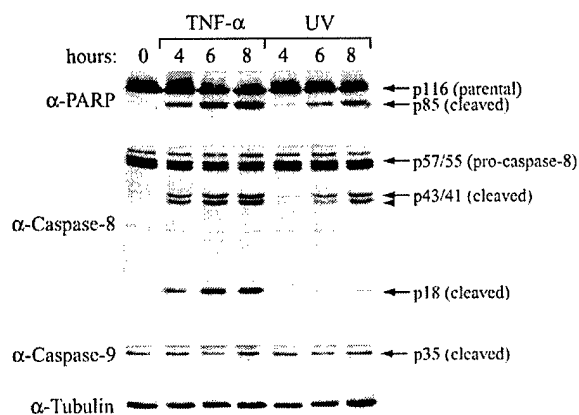
hours: 0 | 4 6 8 | 4 6 8

TNF-α   UV

α-PARP ←p116 (parental)
←p85 (cleaved)

α-Caspase-8 ←p57/55 (pro-caspase-8)
←p43/41 (cleaved)

←p18 (cleaved)

α-Caspase-9 ←p35 (cleaved)

α-Tubulin

Figure 2. TNF-α and UV treatment both result in caspase-8 and PARP cleavage while caspase-9 cleavage is unchanged. To determine if UV treatment can result in activation of the initiator caspase-8, MCF-7 cells were serum starved for 18 hours before treatment with either UV irradiation (10 J/M^2) or TNF-α (100 ng/ml) and cycloheximide (1 µg/ml). At times indicated, cells were harvested. Cell lysates were subjected to SDS-PAGE and Western blot analyses to determine the extent of PARP, caspase-9 and caspase-8. Western analysis of tubulin indicates similar protein loading in each lane.
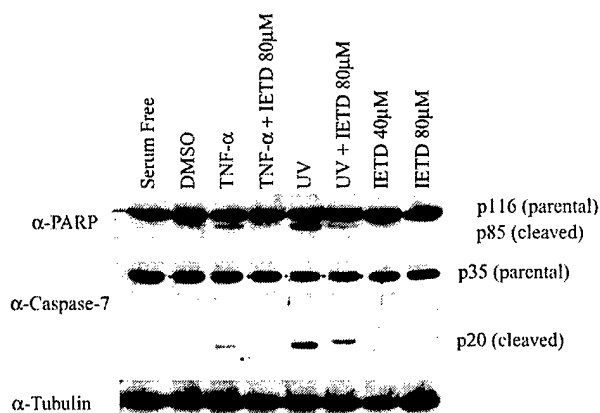

Serum Free | DMSO | TNF-α | TNF-α + IETD 80µM | UV | UV + IETD 80µM | IETD 40µM | IETD 80µM

α-PARP — p116 (parental)
p85 (cleaved)

α-Caspase-7 — p35 (parental)

p20 (cleaved)

α-Tubulin

Figure 3. Inhibition of caspase-8 by Z-IETD-FMK results in reduction of TNF-α and UV induced apoptosis. To investigate the contribution of caspase-8 to apoptosis, MCF-7 cells were pretreated with 80µM Z-IETD-FMK or DMSO only (vehicle control) for 30 minutes prior to treatment with TNF-α (100 ng/ml) or UV irradiation (10 J/M^2). Six hours later cells were harvested, and cell lysates were subjected to SDS-PAGE and Western blot analyses to determine the extent of PARP and caspase-7 cleavage. Western analysis of tubulin indicates similar protein loading in each lane.

In contrast to the MCF-7 cell line, irradiation of the MDA MB-231 breast cancer cells (which expresses mutant p53) induces caspase-9 cleavage and IGF-I co-treatment reduces caspase-9 cleavage (Figure 4). Even though this was our predicted outcome, we see no evidence that Akt inhibits caspase-9 activity through caspase-9 phosphorylation (data not shown). Thus, we are currently testing if IGF-I activated Akt may mediate the ability of XIAP (X-linked inhibitor of apoptosis, an inhibitor of caspase-9) to bind to caspase-9 as another mechanism for the protective effect that we observe (Figure 5).
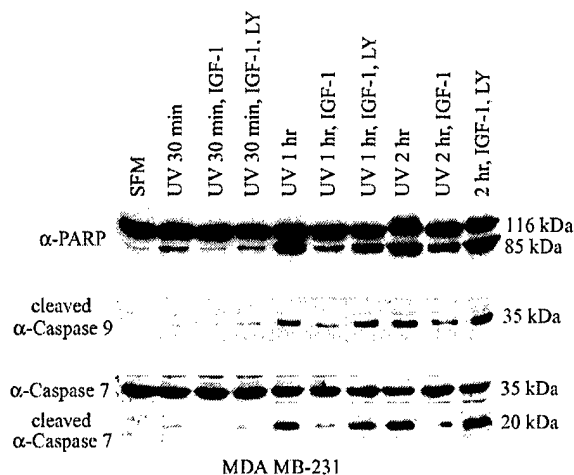

SFM | UV 30 min | UV 30 min, IGF-1 | UV 30 min, IGF-1, LY | UV 1 hr | UV 1 hr, IGF-1 | UV 1 hr, IGF-1, LY | UV 2 hr | UV 2 hr, IGF-1 | 2 hr, IGF-1, LY

α-PARP — 116 kDa
85 kDa

cleaved
α-Caspase 9 — 35 kDa

α-Caspase 7 — 35 kDa

cleaved
α-Caspase 7 — 20 kDa

MDA MB-231

Figure 4. UV treatment leads to caspase-9 cleavge and IGF-I inhibits UV mediated caspase-9 activation. To determine if UV treatment can result in activation of the initiator caspase-9, MDA MB-231 cells were serum starved for 18 hours before treatment with either UV irradiation (0.75 J/M^2) and/or IGF-I (50 ng/ml) and LY294002 (25 µM). At times indicated, cells were harvested. Cell lysates were subjected to SDS-PAGE and Western blot analyses to determine the extent of PARP, caspase-9 and caspase-7 cleavage. Western analysis of tubulin indicates similar protein loading in each lane.
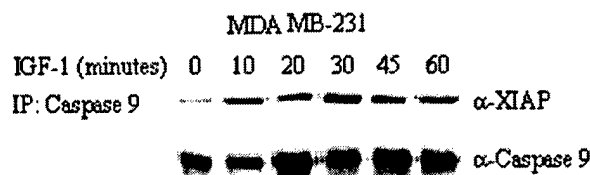
2

MDA MB-231

IGF-1 (minutes)   0   10   20   30   45   60

IP: Caspase 9   ▬ ▬ ▬ ▬ ▬ ▬   α-XIAP

                 ▬ ▬ ▬ ▬ ▬ ▬   α-Caspase 9

Figure 5. IGF-I treatment enhances caspase-9 binding to XIAP. MDA MB 231 cells were plated and serum starved overnight. The following day cells were treated with IGF-I for the indicated times. Cells were lysed at each time point and 200 mcg of protein was immunoprecipitated with a caspase-9 antibody and immune complexes were subjected to SDS-PAGE and later Western blotted for XIAP and caspase-9.

Task 2 is to characterize the potential interactions between the PI 3-kinase survival and stress-induced signaling pathways by exposure to IGF-I and/or chemotherapy and using pharmacologic and molecular techniques to confirm these interactions.

Our interesting observation that IGF-I treatment markedly enhances JNK activity in a PI 3-kinase dependent fashion in MCF-7 cells has recently been a major focus in my lab. We have shown that IGF-I activation of JNK is stronger than that induced by stress treatments such as Taxol or Taxotere chemotherapeutic agents. When cells are co-treated with IGF-I and chemotherapy, JNK activity is further enhanced (in contrast to our prediction) (Figure 6 and reference (1)). Thus, we have been very interested in the biological consequence of JNK activation by growth factors. In the past two years we have made significant progress. We have published a manuscript to *Oncogene* that describes that overexpression of wildtype JNK inhibits anchorage independent growth of MCF-7 cells and IGF-I stimulated anchorage independent growth (1). Initially we hypothesized that IGF-I activation of JNK is resulting in a negative feedback loop. Other investigators have shown in diabetic models that stress treatments such as TNF-α (tumor necrosis factor) enhances JNK activity. Activated JNK then phosphorylates IRS-1 (insulin receptor substrate) on Serine 307. Phosphorylation of this residue inhibits IRS-1 association with insulin and IGF-I receptors, resulting in decreased growth factor mediated signaling. Most recent work in our lab indicates that stress-induction of JNK phosphorylates Ser 307 of IRS. IGF-I also phosphorylates this site in an Akt-dependent fashion. However, neither JNK nor Akt can phosphorylate this site without activation or binding of mTOR to IRS-1 (data not shown). This work will soon be submitted to the *Journal of Biological Chemistry*.
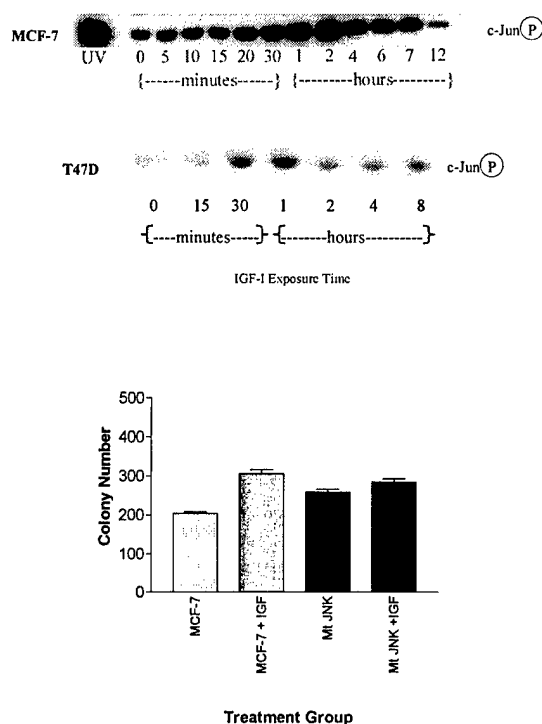
MCF-7 ● ●●●●●●●● ▬ ▬ ▬ ▬   c-Jun(P)
        UV   0   5 10 15 20 30 1   2   4   6   7   12
             {------minutes------} {---------hours---------}

T47D   ▬ ▬ ▬ ▬ ▬ ▬ ▬   c-Jun(P)
        0   15   30   1   2   4   8
        {----minutes----}-{-------hours----------}

IGF-I Exposure Time

Figure 6. JNK activity is dramatically increased with IGF-I treatment in MCF-7 cells. MCF-7 and T47D breast cancer cells were treated with IGF-I (50 ng/ml) in a time-course experiment. *A.* Analyses of phosphorylated c-Jun$_{(1-79)}$ resulting from *in vitro* kinase assays of MCF-7 cells are shown. UV (50 J/M^2) was used as a positive control for JNK activation in MCF-7 cells. *B.* JNK overexpression inhibits anchorage independent growth of MCF-7 cells. Parental MCF-7 cells and stable Wt and Mt JNK transfectant MCF-7 cells were suspended cells in 5% CSS and 0.8% Seaplaque agarose. Cells were seeded at 30,000 per dish and grown for 9 days. IGF-I (50 ng/ml) was added as indicated. Each sample was grown in triplicate and colonies were counted within the same surface area.

Colony Number [bar chart: MCF-7 ≈200, MCF-7 + IGF ≈300, Mt JNK ≈255, Mt JNK +IGF ≈280]

Treatment Group

In November of 2001, we received an $50,000 Avon seed grant to continue our studies of IGF-I activated JNK. The aims of this grant were to identify upstream kinases that mediate IGF-I activation of JNK and to inhibit JNK isoforms to determine if IGF-I activates different JNK isoforms than stress treatments. We are approaching this question through a collaboration with ISIS Pharmaceutical company who have provided us with JNK antisense oligonucleotides.

Task 3 is to characterize if IGF-I and chemotherapy interactions in breast cell lines are p53 dependent and to compare this activity in an ER positive cell line, and ER negative cell line, and an immortalized, noncancerous breast epithelial cell line.

In the DoD grant, I proposed to study both mutant p53 and wildtype p53 expressing breast cancer cell lines. We have done this to some extent but have also had difficulty in deciphering general differences in cell line sensitivity versus differences in mutant versus wildtype p53 function. Using a short inhibitory (si)RNA approach, we have recently shown that JNK's ability to induce cell cycle arrest is independent of p53 in the MCF-7 cells that express wildtype p53 and ER (Figure 7). Most of our other findings also suggest that Akt mediated survival is also independent of p53 expression, as discussed above in Task 1 using the MDA MB-231 cell line which expresses mutant p53. We have also studied the 21PT cell line which expresses a truncated p53 (Figure 7). In this instance, IGF-I protects from apoptosis in a p53-independent fashion (3).

Task 4 is to study IGF-I treatment effects on xenograft breast cancer response to chemotherapy drugs.

We have recently submitted an RO1 application to use established transgenic mouse models and JNK knockout mice to better understand the interactions of JNK with p53, growth factor mediated pathways, and the efficacy of chemotherapy drugs. Based on the literature and our own preliminary data, we hypothesize that loss of JNK activity will *inhibit* mammary tumor development in mice overexpressing the polyoma virus middle T-antigen or lacking p53. Once breast tumors have developed, we then plan to determine if JNK expression is important for efficacy of anti-cancer drugs. We will determine if these effects are JNK gene dependent by using both JNK 1 and JNK 2 knockout mice. The RO1 application will be resubmitted November 1, 2003. If funded, the aims will supplant the current Task 4 of my CDA award. I believe that use of the transgenic and knockout mice will address the same question but provide much more mechanistic information to the initial approach described.
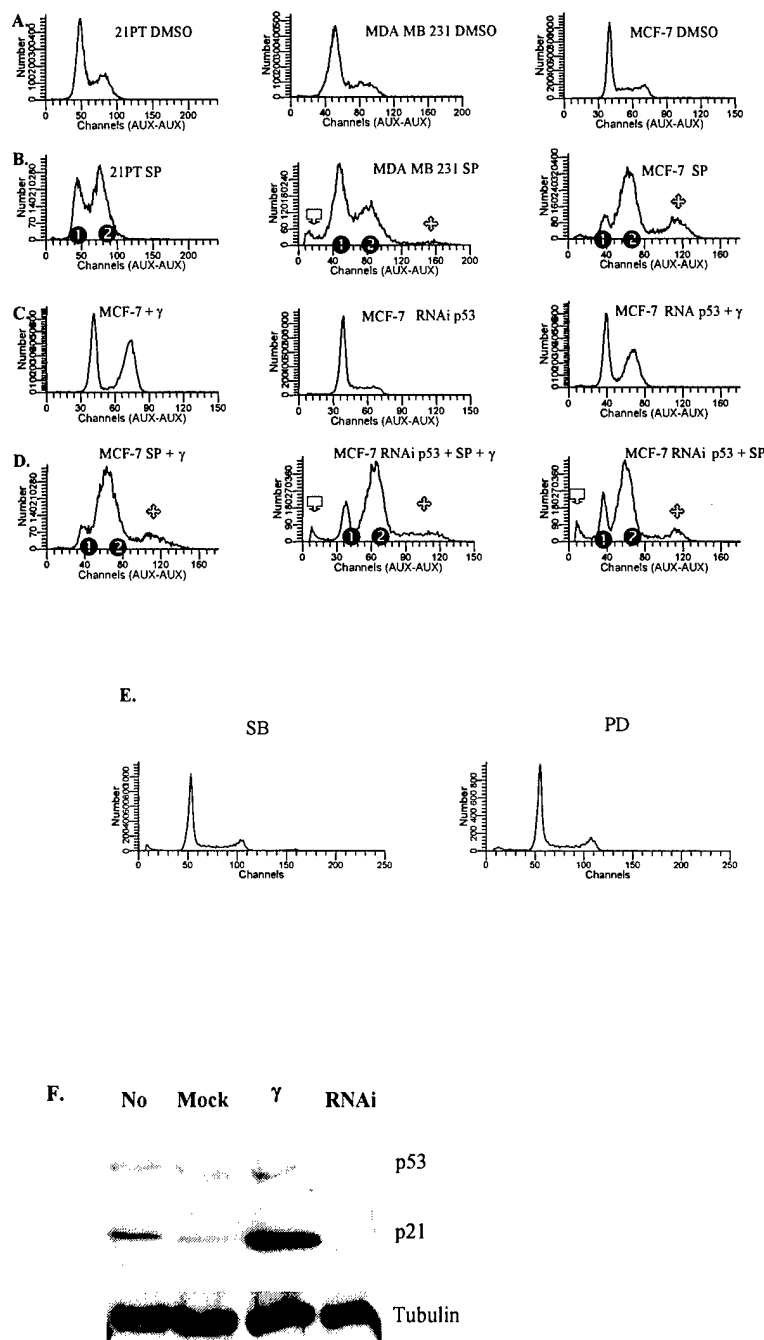
A. 21PT DMSO   MDA MB 231 DMSO   MCF-7 DMSO

B. 21PT SP   MDA MB 231 SP   MCF-7 SP

C. MCF-7 + γ   MCF-7 RNAi p53   MCF-7 RNA p53 + γ

D. MCF-7 SP + γ   MCF-7 RNAi p53 + SP + γ   MCF-7 RNAi p53 + SP

Number / Channels (AUX-AUX)

E.

SB   PD

Number / Channels

Figure 7. Cell cycle distribution of breast cancer cells. Cells were treated with SP 25 µM, siRNA p53 SUPER and/or γ irradiation (6 Gy) and cultured for 48 hours. Cells were then trypsinized, washed with PBS, fixed, and later stained using propidium iodide (PI). DNA content of cells was analyzed by flow cytometry. **A).** Cell cycle histograms of asynchronized, subconfluent 21PT, MDA MB 231, and MCF-7 breast cancer cells. **B).** Cell cycle distributions of 21PT, MDA MB 231, and MCF-7 cells after 48 hours of SP treatment.   sub-G1 cells, ❶ G1 cells, ❷ G2/M cells,   endoreduplicating cells. **C).** MCF-7 cells were either treated with γ irradiated, transfected with p53 siRNA or both, as indicated. **D).** MCF-7 cells were treated with SP and transfected with p53 siRNA or treated with γ irradiation, as indicated. **E).** MCF-7 cells were incubated for 48 hours in SB203580 (SB) or PD98059 (PD), and processed as above. **F).** MCF-7 cells were lysed at indicated time points. 60 µg of total protein lysate were separated by SDS PAGE, transferred to nitrocellulose, then Western blotted with antibodies to the indicated proteins.

F.   No   Mock   γ   RNAi

p53

p21

Tubulin

5

References

1. Mamay, C. L., Mingo-Sion, A. M., Wolf, D. M., Molina, M. D., and Van Den Berg, C. L. An inhibitory function for JNK in the regulation of IGF-I signaling in breast cancer., Oncogene. *22:* 602-14, 2003.
2. Ferguson, H. A., Marietta, P. M., and Van Den Berg, C. L. UV induced apoptosis is mediated independent of caspase 9 in MCF-7 cells- a model for cytochrome *c* resistance., Journal of Biological Chemistry. *278:* 45793-45800, 2003.
3. Mingo-Sion, A. M., Marietta, P. M., Koller, E., and Van Den Berg, C. L. Inhibition of JNK reduces G2/M transit independent of p53, leading to endoreduplication, decreased proliferation and apoptosis in breast cancer cells., Oncogene. *In press:*, 2003.

Training accomplishments

We have had a marked increase in our publication rate in the past two years of this Career Development Award (see below). In regards to funding, Dr. Horwitz (my mentor) has been instrumental in earning the Avon breast cancer foundation award. Seed funds from this award provided support for many of the JNK research currently taking place in my laboratory. This Foundation award has brought breast cancer researchers from the area in closer contact and more collaborative. In regards to my career development, I have also served as a grant reviewer for both DoD and NIH in the past tow to three years. This has given me a great opportunity to stay abreast of breast cancer research and better reflect upon my own research program's focus and progress.

Key Research accomplishments:

1. Characterization of IGF-I activation of JNK inhibits IGF-I responses in breast cancer cells (Years 1-3).
2. Collaboration with ISIS Pharmaceutical company to study JNK isoform specificity of function (Years 2-4).
3. IGF-I survival responses in DNA damaged breast cancer cells are caspase 9 independent but caspase 7 sensitive in MCF-7 cells (Years 3-4).
4. Characterization of the importance of stress-activated and basal JNK activity in breast cancer phenotypes including cell cycle arrest, endoreduplication and apoptosis (Years 2-4).
5. Characterization of mTOR in mediating stress and growth factor mediated phosphorylation of IRS-1 Ser307 (Year 4).
6. Characterization of the importance of mTOR in caspase-8 mediated cell death (Year 4).

Reportable Outcomes:

Grant activity
1. Avon seed grant award
2. NIH/NCI RO1 awarded in June, 2000, entitled, "IGF-I survival effects on p53 induced apoptosis."
3. Submission of grant application to NIH entitled, "The role of JNK in mammary tumorigenesis and response to treatment."
4. Submission of grant application to the Komen Breast Cancer Foundation entitled, "The role of JNK in mammary development and tumorigenesis."

Abstracts

1. Van Den Berg, C.L., Sion, A., Mamay, C.L. Molecular targets for IGF-I protection of irradiated breast cancer cells. Era of Hope. Department of Defense Breast Cancer Research Program Meeting 3:P36-17, 2002.
2. Ferguson, H.A., Marietta, P.M., Van Den Berg, C.L. UV-induced apoptosis occurs independently of the apoptosome in MCF-7 breast cancer cells. Molecular Mechanisms of Apoptosis Keystone Symposia 2003; 164.

Manuscripts:

1. Mamay, C.L., Mingo-Sion, A.M., Wolf, D.M., Molina, M.D., Van Den Berg, C.L. An inhibitory function for JNK in the regulation of IGF-I signaling in breast cancer. Oncogene 2003; 22: 602-14.
2. Ferguson, H.A., Marietta, P.M. Van Den Berg, C.L. UV induced apoptosis is mediated independent of caspase 9 in MCF-7 cells – a model for cytochrome C resistance. Under revision for Journal of Biological Chemistry.
3. Van Den Berg, C.L. IGF-I influence on breast cancer cell survival. Invited review submitted to Breast Diseases.
4. Mingo-Sion, A.M., Marietta, P.M. Koller, E., Van Den Berg, C.L. Inhibition of JNK reduces G2/M transit independent of p53, leading to endoreduplication, decreased proliferation and apoptosis in breast cancer cells. Oncogene In press.
5. Mingo-Sion, A.M., Koller, E., Van Den Berg, C.L. Mammalian target of rapamycin and p70 S6 kinase predominantly regulate insulin receptor substrate-1 Ser312 phosphorylation in breast cancer cells. In preparation.

Conclusions: The past two years of this Career Development have been very productive in characterizing the IGF-I induced pathways and the mechanism(s) of their effects on cellular outcomes. Our findings have lead to one funded RO1, an Avon seed grant, and three other grant applications to NIH, DoD and the Susan G Komen. Our research on Akt is leading us to new mechanisms for IGF-I mediated protection. Our work on JNK is allowing us to further determine if activation of this kinase that JNK activation inhibits IGF-I responses and that JNK activity mediates chemotherapy induced cell death provides us with a very promising target for therapeutic interventions. We first would like to confirm and extend our JNK and Akt studies using animal models, thus we have grant applications pending to do such studies. Currently, I have five publications that my DOD Career Development has supported, in part.

UV-induced Apoptosis Is Mediated Independent of Caspase-9 in MCF-7 Cells

A MODEL FOR CYTOCHROME c RESISTANCE*

Heather A. Ferguson, Peter M. Marietta, and Carla L. Van Den Berg‡

From the School of Pharmacy, University of Colorado Health Sciences Center, Denver, Colorado 80262

The importance of the mitochondria in UV-induced apoptosis has become increasingly apparent. Following DNA damage cytochrome c and other pro-apoptotic factors are released from the mitochondria, allowing for formation of the apoptosome and subsequent cleavage and activation of caspase-9. Active caspase-9 then activates downstream caspases-3 and/or -7, which in turn cleave poly(ADP)-ribose polymerase (PARP) and other downstream targets, resulting in apoptosis. In an effort to understand the mechanisms of Akt-mediated cell survival in breast cancer, we studied the effects of insulin-like growth factor (IGF)-I treatment on UV-treated MCF-7 human breast cancer cells. Apoptosis was induced in MCF-7 cells after UV treatment, as measured by caspase-7 and PARP cleavage, and IGF-I co-treatment protected against this response. Surprisingly caspase-9 cleavage was unchanged with UV and/or IGF-I treatment. Using MCF-7 cells overexpressing caspase-3 we have shown that resistance of caspase-9 to cleavage was not altered by the expression of caspase-3. Furthermore, overexpression of caspase-9 did not enhance PARP or caspase-7 cleavage after UV treatment. Because caspase-8 was activated with UV treatment alone, we believe that UV-induced apoptosis in MCF-7 cells occurs independently of cytochrome c and caspase-9, supporting the existence of a cytoplasmic inhibitor of cytochrome c in MCF-7 cells. We anticipate that such inhibitors may be overexpressed in cancer cells, allowing for treatment resistance.

Caspases, a family of cysteine proteases, are an integral part of the execution phase of programmed cell death. Initiator caspases-2, -8, -9, and -10 are first induced to undergo oligomerization, leading to autocatalytic activity and subsequent cleavage of the downstream effector caspases (see Refs. 1 and 2 for review). The two major pathways for the execution of apoptosis are defined by the initiator caspases-8 and -9. Caspase-8-induced apoptosis is regulated via activation of the tumor necrosis factor (TNF)[1] receptor superfamily of receptors in-

duced by ligands such as TNF-α, TRAIL, or Fas (3, 4). Proteolytically activated caspase-8 then cleaves effector caspases-3 and -7 (5, 6). Caspase-8 can also cleave Bid to its truncated form (tBid) (7). tBid translocation to mitochondria induces mitochondrial release of cytochrome c and subsequent activation of caspase-9, thus amplifying the death signal.

Non-cytokine-mediated cellular stress, such as UV or chemical treatment, can initiate apoptosis through mitochondrial release of cytochrome c (8). In the caspase-9 initiated pathway, cytoplasmic cytochrome c triggers the formation of the apoptosome, a multi-protein complex containing cytochrome c, dATP, Apaf-1, and pro-caspase-9 (9, 10). The presence of caspase-3 and/or -7 within the apoptosome may allow more optimal cleavage of caspase-9. Ultimately, activated caspase-9 serves as the initiator caspase, which may further amplify an apoptotic signal by activating caspase-8 and -2 upstream of the mitochondria (11). Downstream responses to caspase-9 include cleavage of caspase-3 and/or -7 and eventually poly(ADP)-ribose polymerase (PARP) (12).

Multiple mechanisms of resistance to apoptosis have been recently identified. By phosphorylating caspase-9, Akt inhibits its proteolytic activity (13). Further, resistance to mitochondrial initiated events has also been reported. For example, Bcl-2 and Bcl-XL can inhibit cytochrome c translocation (14–16). Bcl-XL may also participate in binding to the apoptosome to inhibit its activity (14, 17, 18). The apoptosome and effector caspase activity can be further regulated by members of the IAP (inhibitor of apoptosis proteins) family of proteins, which can directly bind to caspases via BIR (baculoviral IAP repeat) protein domains. BIR domains 1 and 2 of IAPs bind and inhibit caspases-3 and -7, whereas the BIR3 domain binds to and specifically inhibits caspase-9 (19, 20). These inhibitory effects can be offset by the stress-induced release of the mitochondrial protein, Smac/Diablo, which competitively binds to IAPs, relieving their inhibitory effects on caspases-3, -7, and -9 (21, 22). Aberrations of Apaf-1 can also inhibit caspase-9 response. Methylation mediated transcriptional repression of Apaf-1 has been reported in metastatic melanomas and ovarian cancer cell lines (23, 24), whereas reconstitution of Apaf-1 expression enhances apoptotic response to the chemotherapeutic drug doxorubicin (23).

Akt mediates survival by phosphorylating several substrates that are intimately involved in regulating programmed cell death. Akt phosphorylation of pro-caspase-9, a downstream target of p53, blocks cleavage of pro-caspase-9 and its subsequent activation (13, 25). Thus, regulation of pro-caspase-9 is of particular importance in p53-mediated effects. Therefore, we initially set out to determine whether pro-caspase-9 may be an Akt target for survival of IGF-I sensitive breast cancer cells.

Since the discovery that MCF-7 human breast cancer cells do not express full-length caspase-3, because of a 47-base pair

[1] The abbreviations used are: TNF, tumor necrosis factor; PARP, poly(ADP)-ribose polymerase; PBS, phosphate-buffered saline; Z-IETD-FMK, Z-Ile-Glu-(OMe)-Thr-Asp(OMe) fluoromethyl ketone.

deletion within exon 3 of the caspase-3 gene, debate has existed regarding the ability of MCF-7 cells to undergo programmed cell death (26, 27). More recently, the MCF-7 cell line has become a model for investigation of caspase-3-dependent and -independent effects. Although less studied, caspase-7 may convey many of the same effects as caspase-3, suggesting some redundancy between the two proteins. Here we show that MCF-7 cells undergo caspase-mediated apoptosis upon UV treatment, as indicated by caspase-7 and PARP cleavage. Most interesting is our observation that UV treatment can induce apoptosis via caspase-8 activation, independent of caspase-9. Additionally, in studying the potential mechanism for the lack of a caspase-9 response, we conclude that MCF-7 cells harbor a cytochrome c or apoptosome defect.

EXPERIMENTAL PROCEDURES

Cell Culture and Treatments—MCF-7 cells were provided by Dr. C. Kent Osborne (University of Texas Health Science Center, San Antonio, TX), and other MCF-7 cells were provided by Dr. Heide Ford (University of Colorado Health Sciences Center, Denver, CO); HEK 293 cells were provided by Dr. Douglas Wolf (University of Colorado Health Sciences Center, Denver, CO). Cell lines were maintained in full serum medium (MCF-7 in Iscove's modified Eagle's medium (Mediatech, Herndon, VA) supplemented with 10% fetal bovine serum (Mediatech), antibiotics, and insulin; HEK 293 in Dulbecco's modified Eagle's medium (Mediatech) was supplemented with 10% fetal bovine serum (Mediatech) and antibiotics). In each experiment the cells were plated in full serum-containing media and cultured overnight at 5% CO_2 and 37 °C. The cells were washed twice the next day in warm phosphate buffered saline (PBS; Biofluids, Rockville, MD) followed by overnight culture in serum-free medium. On the third day, the cells were treated with UV (UV-C, 10 J/m²) in a SpectroLinker UV linker 100 (Spectronics, Westbury, NY) with lids removed and/or IGF-1 (obtained from the National Hormone and Pituitary Program, NIDDK, National Institutes of Health and Dr. A. F. Parlow) or with TNF-α (Alexis Biochemicals, San Diego, CA) and cycloheximide (Sigma-Aldrich), as indicated in figure legends. When applicable, pretreatments with LY294002 (Alexis Biochemicals) or Z-IETD-FMK (BD Pharmingen, San Diego, CA) were performed 40 or 30 min prior to stimulation with UV, respectively.

Stable and Transient Transfections—pcDNA3 caspase-3 and FLAG-caspase-9 vectors were graciously provided by Dr. C. Vincenz (University of Michigan). Generation of MCF-7 caspase-3 stable transfectants was performed by electroporation of 3.0×10^6 MCF-7 cells in 200 μl of medium containing 10 μg of DNA. Forty-eight hours later, the cells were selected with 800 μg/ml of G418 (Mediatech). Individual drug-resistant colonies were isolated and expanded. Detection of clones overexpressing caspase-3 was performed by Western blot analysis using a caspase-3 antibody (Santa Cruz Biotechnology, Santa Cruz, CA).

For transient transfections with wild-type caspase-9 or Bcl-2, 1.0×10^6 MCF-7 cells were plated in 6-cm² dishes and cultured overnight in full serum medium. The cells were washed twice the following day with warm PBS and then incubated with serum free Opti-MEM (Invitrogen) for 45 min at 37 °C and 5% CO_2. The cells were then transfected with 30 μl of Plus reagent, 4 μl of LipofectAMINE (Invitrogen), and 4 μg of DNA (3 μg of DNA of interest and 1 μg of green fluorescent protein); 3 h later plates were supplemented with full serum medium. Twenty-four hours after transfection the cells were assessed for transfection efficiency by visualization of green fluorescent protein and then treated as mentioned above.

Preparation of Cell Lysates and Western Blot Analyses—At the indicated times, the cells were scraped and harvested by centrifugation. The plates were washed once with cold PBS followed by an additional centrifugation. The cells were then lysed in lysis buffer (20 mM Tris-HCl, 250 mM NaCl, 3 mM EDTA, 0.05% Nonidet P-40, 1 mM dithiothreitol, 0.368 mg/ml Na Orthovanadate, 5 μg/ml leupeptin, 1 mM phenylmethylsulfonyl fluoride, and 17 μg/ml aprotinin) followed by centrifugation at 13,000 to remove cellular debris. The protein concentrations were determined using a Bio-Rad D/C protein assay kit. Sixty micrograms of total cell lysate were resolved by 10% SDS-PAGE, unless stated otherwise, and transferred to nitrocellulose. Western blot analyses were performed using primary antibodies for caspase-3, caspase-7, caspase-8, caspase-9, cleaved caspase-9 D315 (Cell Signaling, Beverly, MA), PARP (BD Pharmingen), XIAP (BD Pharmingen), or tubulin (Sigma), and enhanced chemiluminescence (Applied Biosystems, Foster

City, CA). Each Western blot shown is representative of at least three separate experiments.

Antibody Cross-linking and Immunoprecipitations—Immunoprecipitations were performed by first cross-linking antibody to protein G-agarose beads (Invitrogen). The antibody for caspase-9 (Santa Cruz Biotechnology) was incubated with protein G-agarose beads in PBS for 3 h at 4 °C. The beads were washed six times in 0.18 M sodium borate (pH 8.0) before incubation with 0.18 M sodium borate (pH 8.0) containing 100 mM DMP (dimethylpimelimidate) for 2 h at room temperature. The beads were then washed three times with 0.2 M ethanolamine and incubated with 0.2 M ethanolamine for 2 h at room temperature. The cross-linked beads were washed in cold PBS and stored at 4 °C.

For immunoprecipitations, the cells were treated and harvested as described above. For each treatment, 200 μg of total cell lysate were incubated with 10 μl of cross-linked beads in a total volume of 300 μl of lysis buffer. Incubation was carried out for 3 h at 4 °C; beads were then washed three times with lysis buffer before being resolved by 10% SDS-PAGE. Western blots were carried out as described above.

Mitochondrial Inner Membrane Potential—Mitochondrial inner membrane potential was assessed by a mitochondrial voltage-sensitive dye JC-1 (Intergen, Purchase, NY) per manufacturer instructions and flow cytometry (FACSCalibur, Becton Dickinson, University of Colorado Cancer Center Flow Cytometry Core facility, which is supported by NCI, National Institutes of Health Cancer Core Support Grant CA46934). The fluorescent mitochondrial probe, JC-1, was used to verify treatment mediated changes in mitochondrial membrane $\Delta\psi$. In apoptotic cells, the JC-1 dye remains monomeric in the cytoplasm showing green fluorescence. Whereas in unstressed cells, the mitochondrial aggregate forms fluorescent red at 590 nm. The experiments were repeated three times, and representative results are shown.

Cytochrome c Immunostaining—The cells were plated at a density of 85,000 cells/25-mm diameter slides (Lab-Tek, Nalge Nunc, Naperville, IL) and fixed in PBS containing 2% paraformaldehyde. The cells were washed in PBS, permeabilized in 0.2% Triton X-100, and then blocked in 10% normal goat serum/PBS. The cells were incubated with cytochrome c antibody (clone 6H2.B4 (Pharmingen, San Diego, CA)) and then washed and incubated with mouse IgG Alexa Fluor 488 AB (Molecular Probes, Eugene, OR). The slides were imaged on a Nikon Diaphot TE200 microscope using a CoolSNAP-fx monochrome digital camera and Image-Pro Plus V4.1 software. The images are shown with color overlay. The experiments were repeated three times, and representative results are shown.

In Vitro Cleavage of Pro-caspase-9—A plasmid containing cDNA encoding pro-caspase-9 (pcDNA3-FLAG-tagged caspase-9) was *in vitro* transcribed and translated in the presence of [³⁵S]methionine (Amersham Biosciences) using a coupled transcription/translation TnT kit (Promega, Madison, WI) according to the manufacturer's instructions. The protein was desalted and exchanged into buffer A (20 mM Hepes, pH 7.5, 10 mM KCl, 1.5 mM $MgCl_2$, 1 mM EDTA, and 1 mM dithiothreitol) with Bio-Spin P-6 columns (Bio-Rad). The cell lysates were prepared as described above but were lysed with buffer A. The radiolabeled reactions consisted of 80 μg of cell lysate, 5 μl of ³⁵S-labeled pro-caspase-9, 1.5 mM dATP (Sigma-Aldrich), and 1.8 or 18.0 μM horse heart cytochrome c (Sigma-Aldrich) in a 30-μl total volume; the reactions for Western blot analysis were identical with the omission of ³⁵S-labeled pro-caspase-9. The reactions were allowed to proceed for 4 h at 30 °C before being analyzed by SDS-PAGE and autoradiography (STORM 860, Molecular Dynamics, Amersham Biosciences) or Western blot (19). The experiments were repeated a minimum of two times, and representative results are shown.

Cytochrome c Sequencing—RNA was extracted from confluent 10-cm² dishes of MCF-7 and HEK 293 cells using RNAwiz isolation reagent (Ambion, Austin, TX) per manufacturer instructions. 1 μg of RNA was reverse transcribed with Moloney murine leukemia virus reverse transcriptase (Invitrogen) in 20 μl of reaction mixture. Cytochrome c was amplified from the resulting cDNA (10 μl) using platinum *Pfx* DNA polymerase (Invitrogen) and the primers 5'-gagtgttcgttgtgccagcg and 5'-gcccaacaaaatattctgtcagtc. cDNA was amplified in 35 cycles, consisting of denaturing for 15 s at 94 °C, annealing for 30 s at 55 °C, and primer extension for 60 s at 68 °C. The PCR products were purified using Microcon PCR Centrifugal Filter devices (Ambion) per manufacturer instructions. The University of Colorado Cancer Center DNA Sequencing and Analysis Core Facility, which is supported by NCI, National Institutes of Health Cancer Core Support Grant CA46934, sequenced the DNA samples using an ABI Prism 3100 capillary automated sequencer (Applied Biosystems). Analyses of DNA sequences were done with Sequencher 3.1 (Gene Codes Corp., Ann Arbor, MI).
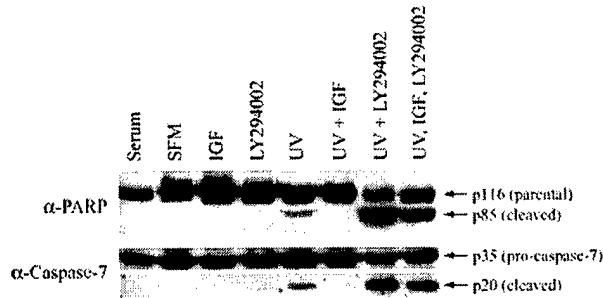
FIG. 1. **UV induced PARP and caspase-7 cleavage can be inhibited by IGF-I effects on phosphatidylinositol 3-kinase.** MCF-7 cells were plated and serum-starved as described under "Experimental Procedures." The following day cells were treated with UV irradiation (10 J/m²) with or without IGF-I co-treatment (50 ng/ml). Where indicated, the cells were exposed to 50 μM LY294002 for 40 min prior to UV irradiation and/or IGF-I treatment. The cells were lysed 6 h after UV and/or IGF-I treatment. The cell lysates were then subjected to Western blot analyses to detect parental or cleavage forms of PARP and caspase-7. The presence of the 85-kDa PARP and 20-kDa caspase-7 cleavage fragments indicate induction of apoptosis. *SFM*, serum-free medium.

RESULTS

UV Induces Caspase-7 and PARP Cleavage in MCF-7 Cells— Because UV irradiation frequently induces mitochondrial release of cytochrome c and cleavage of caspase-9, we exposed MCF-7 breast cancer cells to UV irradiation to induce apoptosis via PARP and caspase-7 cleavage and also to determine whether IGF-I co-treatment could inhibit UV-mediated cell death. We also pretreated cells with LY294002, which blocks the activity of phosphatidylinositol 3-kinase and downstream Akt. Measurement of PARP cleavage was used as a direct measure of apoptosis. Fig. 1 clearly shows that MCF-7 cells that are induced to undergo apoptosis via UV irradiation are protected by co-treatment with IGF-I, and this survival effect can be blocked by LY294002. Because MCF-7 cells are deficient in caspase-3, we also measured caspase-7 processing to determine whether it could function similarly to caspase-3 as an effector caspase that can cleave PARP (Fig. 1). Caspase-7 cleavage patterns were very similar to those of PARP, in that UV treatment resulted in caspase-7 cleavage, and IGF-I co-treatment inhibited its cleavage. These data support a previous study showing that caspase-7 catalytic activity can induce PARP cleavage (28). By assessing both caspase-7 and PARP cleavage, LY294002 not only reversed IGF-I-mediated survival, but it also enhanced cell death in the presence of UV irradiation, presumably by inhibiting survival signals mediated by phosphatidylinositol 3-kinase.

Caspase-9 Cleavage Is Unchanged with UV and/or IGF-I Treatment— UV irradiation induces apoptosis among various cell types in a mitochondrial-dependent manner (8). Following irradiation, cytochrome c is released from the mitochondria into the cytosol, where it then complexes with Apaf-1, dATP, and pro-caspase-9 to form the apoptosome. Once bound in the apoptosome, pro-caspase-9 is processed to its active form, and it then activates effector caspases-3 and -7 to complete the apoptotic process. We sought to determine whether pro-caspase-9 is processed as expected in our MCF-7 cells and whether IGF-I could inhibit pro-caspase-9 cleavage. Again, UV treatment of MCF-7 cells induced PARP cleavage (Fig. 2). Despite the UV-induced PARP cleavage, we observed no detectable changes in the amount of caspase-9 cleavage following UV treatment. Also intriguing was the amount of caspase-9 cleavage present in the absence of stress (Fig. 2, *Serum lane,* negative control). Under normal conditions, pro-caspase-9 is not processed unless a stress signal induces cells to undergo apoptosis. In MCF-7 cells,
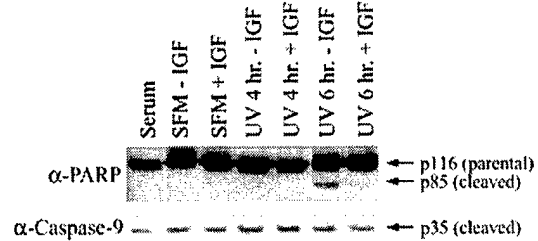

FIG. 2. **UV-induced apoptosis and IGF-I-mediated survival effects are caspase-9-independent.** MCF-7 cells were plated and serum-starved as described under "Experimental Procedures." The following day cells were treated with UV irradiation (10 J/m²) with or without IGF-I co-treatment (50 ng/ml). Six hours after treatment, the cells were harvested, and the lysates were subjected to Western blot analyses for PARP and pro-caspase-9 cleavage. *SFM,* serum-free medium.

pro-caspase-9 is processed to a small extent even in unstressed cells. We confirmed that the cleavage product observed in MCF-7 cell lysates corresponded to the manufacturer's positive lysate control and not the negative lysate control, ruling out the possibility that we were only detecting a nonspecific band (data not shown). Caspase-9 cleavage was also unaltered by IGF-I treatment, even though the cells were protected from apoptosis (compare PARP cleavage minus and plus IGF-I treatment).

Caspase-3 Expression Does Not Sensitize Caspase-9 to UV Treatment in MCF-7 Cells— The presence of some caspase-9 cleavage in untreated cells and the lack of a caspase-9 treatment-mediated increase in cleavage both suggest either a defect in endogenous pro-caspase-9 or the cellular machinery that processes it. We reasoned that if endogenous pro-caspase-9 of MCF-7 cells is defective, then transfected wild-type pro-caspase-9 could rescue the defect in caspase processing and should further enhance cleavage of the effector caspase-7. Because there is evidence to support a requirement for caspase-3 in the apoptosome for proper function (29), we also decided to address the role of caspase-3 in our model. To distinguish between these two possibilities, we transfected MCF-7 cells with wild-type pro-caspase-9 and reassessed caspase-9 cleavage in the presence and absence of UV irradiation (Fig. 3). Further, because a lack of endogenous caspase-3 could lead to a defect in apoptosome function and subsequent caspase-9 processing, we assessed caspase-9 cleavage in MCF-7 cells stably expressing wild-type caspase-3. As shown in Fig. 3A, transiently transfected pro-caspase-9 is partially processed in MCF-7 cells; however, it does not lead to enhanced processing of effector caspase-7 after UV treatment. Fig. 3B illustrates that caspase-9 cleavage products increase with transfection even in the absence of UV-induced stress. Together, these studies indicate that endogenous pro-caspase-9 is processed in a similar fashion as transfected wild-type protein, ruling out a defect in endogenous caspase-9 in MCF-7 cells and supporting the possibility that UV-mediated apoptosis in MCF-7 cells is caspase-9-insensitive. These data suggest an apoptosome defect in MCF-7 cells.

Other investigators have shown that overexpression of caspase-3 in MCF-7 cells enhances cleavage of pro-caspase-9 by using *in vitro* reactions with exogenous pro-caspase-9 and cytochrome c (27). Although the presence of caspase-3 is evident in the caspase-3 transfectants used in Fig. 3A (data not shown), processing of endogenous caspases-9 and -7 were unaffected by the presence of caspase-3 compared with parental MCF-7 cells. Again, these data indicate that the defect lies upstream of apoptosome formation, not within endogenous pro-caspase-9.

Stress Treatments Induce Cytochrome c Translocation in MCF-7 Cells— Because the initiator caspase-8 can also cleave Bid to tBid and tBid translocation can induce cytochrome c
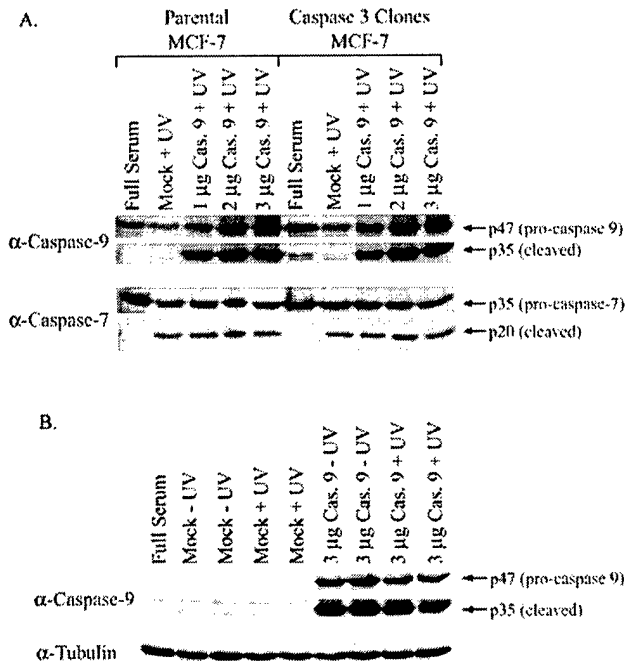
A.

Parental MCF-7   Caspase 3 Clones MCF-7

α-Caspase-9   ← p47 (pro-caspase 9)
     ← p35 (cleaved)

α-Caspase-7   ← p35 (pro-caspase-7)
     ← p20 (cleaved)

B.

α-Caspase-9   ← p47 (pro-caspase 9)
     ← p35 (cleaved)

α-Tubulin

FIG. 3. **Overexpression of caspase-3 or -9 does not enhance UV-mediated apoptosis in MCF-7 cells.** Parental MCF-7 cells and caspase-3 stable transfectants were transiently transfected with increasing amounts of pro-caspase-9 as described under "Experimental Procedures." 24 h after transfection the cells were irradiated (10 J/m²) and then harvested 6 h later. *A*, cell lysates were subjected to SDS-PAGE and Western blot analyses to determine the extent of pro-caspase-7 (p35) processing to a p20 fragment. The treatment-induced appearance of the p20 cleaved caspase-7 fragment indicates induction of apoptosis. *B*, pro-caspase-9 (p47) expression and cleavage to a p35 fragment was assessed with and without UV treatment. Western analysis of tubulin indicates protein loading in each lane.

release, we then tested whether there may be either an aberration in mitochondrial function, preventing proper release of cytochrome *c*, or a defect in the formation and/or function of the apoptosome. Using the JC-1 assay, we first sought to determine whether cellular stress results in mitochondrial membrane depolarization. Further, we wanted to determine whether cytochrome *c* is properly localized and released from mitochondria following UV irradiation. As a positive control for these assays, we used HEK 293 cells. Many investigators have confirmed that UV induces mitochondrial membrane changes and cytochrome *c* translocation in these cells. In the JC-1 assay, we used valinomycin treatment that generally induces mitochondrial membrane Δψ changes in ~95–98% of either HEK 293 or MCF-7 cells (Fig. 4A). Although UV treatment also changed mitochondrial membrane Δψ, it was not as robust as with valinomycin treatment in either cell line. Next, we also examined cytochrome *c* cellular localization using cytochemistry. With this assay we observed that in untreated MCF-7 cells, cytochrome *c* was somewhat diffusely localized in the cytoplasm, whereas the pattern of staining was more characteristic of a mitochondrial, punctate staining in the HEK 293 cells (Fig. 4B). With UV or valinomycin exposure, cytochrome *c* becomes diffusely localized in the cytoplasm in both cell lines. These studies confirm that like HEK 293 cells, MCF-7 cells can respond to cellular stress by changing mitochondrial membrane Δψ and inducing cytochrome *c* cytoplasmic translocation.

MCF-7 Cell Lysates Can Cleave Caspase-9 with Exogenous Cytochrome c—Given our evidence that cytochrome *c* release is stimulated by either valinomycin or UV in MCF-7 cells yet caspase-9 is unresponsive to treatment, we decided to determine whether the defect in pro-caspase-9 processing lies within

the endogenous cytochrome *c* protein itself. Both MCF-7 and HEK 293 cell lysates were obtained from either untreated cells or cells exposed to valinomycin (to stimulate endogenous cytochrome *c* release) prior to harvesting. We then performed *in vitro* caspase-9 cleavage assays (Fig. 5A). Wild-type pro-caspase-9 was *in vitro* transcribed and translated in the presence of [³⁵S]methionine; this protein was then incubated with 80 μg of MCF-7 or HEK 293 cell lysates described above. Exogenous cytochrome *c* was added to some reactions (as indicated) as a positive control to ensure the presence of functional, wild-type cytochrome *c*. The reactions were allowed to proceed for 4 h at 30 °C before being subjected to SDS-PAGE and autoradiography. Untreated MCF-7 and HEK 293 cell lysates do not cleave ³⁵S-labeled pro-caspase-9 (Fig. 5A). When *exogenous* cytochrome *c* and dATP were added to the lysates, caspase-9 cleavage increased proportionate to the concentration of cytochrome *c* present in the reactions. Lysates from valinomycin-treated HEK 293 cells led to the presence of endogenous cytochrome *c* in the reaction and pro-caspase-9 cleavage, comparable with lysates treated with 18 μM cytochrome *c*. In stark contrast, lysates from MCF-7 cells treated with valinomycin did not induce cleavage of caspase-9, even though endogenous cytochrome *c* levels were comparable with those seen in the HEK 293 valinomycin-treated cells. The observation that pro-caspase-9 can be cleaved only when exogenous cytochrome *c* is added to MCF-7 cell lysates suggests that endogenous Apaf-1 is functioning normally to form the apoptosome and that caspase-9 cleavage resistance results from an aberration in the endogenous cytochrome *c* of MCF-7 cells.

We then wanted to confirm our results indicating that endogenous cytochrome *c* cannot induce apoptosome formation and subsequent cleavage of pro-caspase-9. Further, we wanted to determine whether endogenous pro-caspase-9 cleavage can be enhanced when exogenous cytochrome *c* is added. To this end, the same reactions were performed as in Fig. 5A but in the absence of *in vitro* [³⁵S]methionine-labeled pro-caspase-9. In this instance, endogenous cleaved caspase-9 and cytochrome *c* in each reaction were analyzed by Western blot after performing the same reaction conditions as described for Fig. 5A. As illustrated in Fig. 5B, caspase-9 cleavage only occurred in MCF-7 lysates that contain exogenous cytochrome *c*. In contrast, HEK 293 cell lysates were capable of processing pro-caspase-9 when either endogenous or exogenous cytochrome *c* was present in the reactions, as confirmed by Western blotting with an antibody specific for cytochrome *c* (Fig. 5B). Because MCF-7 breast cancer cells may vary from source to source as a result of *in vitro* culturing conditions, we decided to obtain MCF-7 cells from an outside source to assess whether our observations can be generalized. Although a more punctate pattern of cytochrome *c* was observed by cytochemical analysis, we confirmed that the other MCF-7 cells showed an identical pattern of caspase-9 cleavage as our original MCF-7 cells (data not shown).

The ability of MCF-7 cells to process pro-caspase-9 only in the presence of exogenous cytochrome *c* indicates either a defect in the endogenous cytochrome *c* protein or the presence of an inhibitor specific to cytochrome *c* that can be overcome by the addition of excess protein. Thus, cytochrome *c* was sequenced using a reverse transcription-PCR-generated product from MCF-7 cells and compared with the human, wild-type cytochrome *c*. No mutations or truncations were observed in the MCF-7-derived cytochrome *c* (data not shown), confirming its wild-type sequence and further supporting the function of a cytoplasmic, cytochrome *c* inhibitor expressed in MCF-7 breast cancer cells.

A.

FIG. 4. **UV and valinomycin treatments result in changes in mitochondrial membrane potential and cytochrome c translocation.** *A*, HEK 293 and MCF-7 cells were plated. The following day cells were either exposed to UV (20 J/m²) or valinomycin (100 nM) and harvested either 4 h or 15 min later, respectively. Mitochondrial inner membrane potential was assessed using the JC-1 with flow cytometry. In apoptotic cells, the JC-1 dye remains in the cytoplasm showing *green* fluorescence in its monomeric form. Whereas in unstressed cells, the mitochondrial aggregate forms fluoresce *red* at 590 nm. *B*, cells were plated and processed as described under "Experimental Procedures." The cells were incubated with anti-cytochrome *c* followed by Alexa Fluor 488 secondary antibody. The cell images were captured using a monochrome digital camera. The images are shown with color overlay.

B.
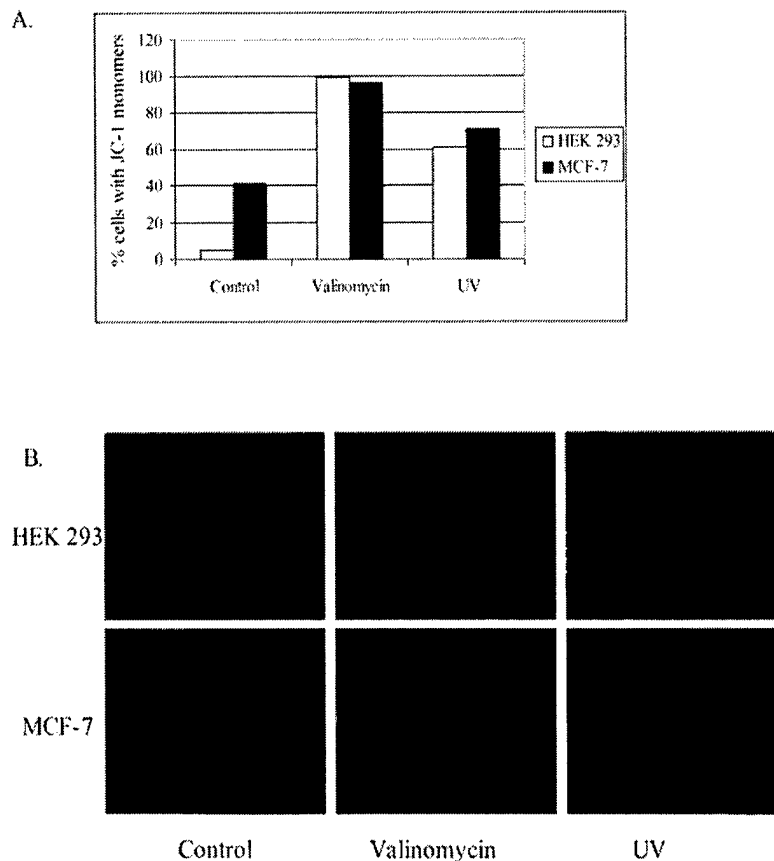
Overexpression of Bcl-2 Does Not Inhibit UV-mediated Apoptosis—Our results thus far indicated that MCF-7 cells do not utilize the intrinsic pathway for UV-mediated apoptosis. We wanted to use other approaches to confirm these observations and also to assess what point in the pathway contributes to a lack of caspase-9 activity. Bcl-2 function is a critical inhibitor of the intrinsic pathway in two potential ways. First, Bcl-2 (and Bcl-XL) can homodimerize to inhibit apoptosis by maintaining mitochondrial membrane potential in the presence of an apoptotic stimuli (15, 16). Second, Bcl-2 (and Bcl-XL) can bind within the apoptosome to inhibit its function (17, 18, 30). To begin these studies untransfected MCF-7 cells were treated with UV and compared with MCF-7 cells that were transfected with either empty vector or vector containing Bcl-2 and then later treated with TNF-α or UV. Again, caspase-7 cleavage was used as a measure of apoptosis. Fig. 6A shows that mock transfected cells were slightly more sensitive to apoptosis compared with untransfected control cells. Cells transfected with Bcl-2 experienced a modest degree of protection from both TNF-α- and UV-mediated apoptosis when overexpressing Bcl-2 compared with the mock transfected cells. Bcl-2 and α-tubulin Western blot analyses confirmed Bcl-2 overexpression of transfectants and even loading of each sample, respectively. These data again indicate that the intrinsic pathway does not significantly contribute to UV-mediated apoptosis.

XIAP Binding to Caspase-9 Is Unaltered by UV Treatment— Recent attention has focused on XIAP binding and inhibition of caspase-9 activity as an important mechanism for caspase-9 resistance to apoptotic stimuli. Therefore, we decided to evaluate whether XIAP may be contributing to caspase-9 resistance. We were unsuccessful at using XIAP as an siRNA target to determine whether inhibition of XIAP would lead to caspase-9 sensitivity, thus we tested whether binding XIAP to
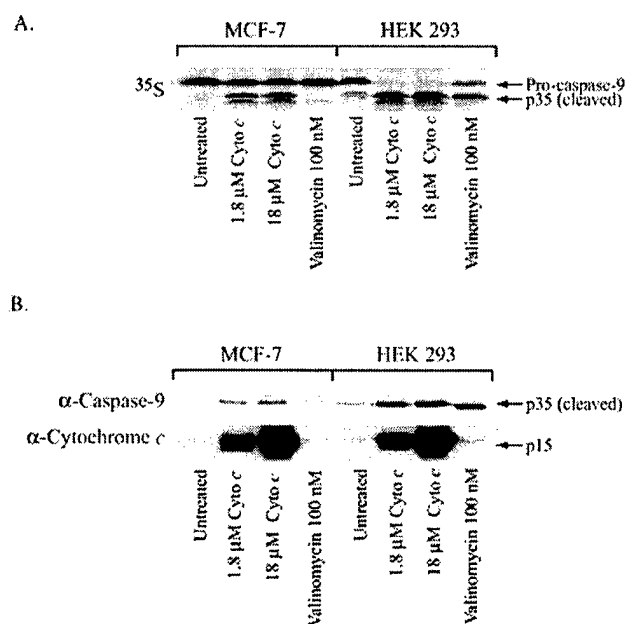
A.

B.

FIG. 5. **MCF-7 cells cleave pro-caspase-9 in the presence of exogenous cytochrome c.** *A*, pro-caspase-9 was *in vitro* transcribed and translated in the presence of [³⁵S]methionine as described under "Experimental Procedures." The protein was incubated with 80 μg of cell lysates from MCF-7 or HEK 293 cells with or without cytochrome (*Cyto*) *c* for 4 h at 30 °C. Different amounts of cytochrome *c* were added as indicated. The reactions were then subjected to 15% SDS-PAGE and autoradiography. *B*, reactions were assembled as described in *A* except for the omission of any exogenous pro-caspase-9. Endogenous cleaved caspase-9 and cytochrome *c* (endogenous or exogenous) were analyzed by 15% SDS-PAGE followed by Western blot analyses.

FIG. 6. Bcl-2 overexpression does not affect UV-mediated apoptotic responses, and XIAP binding to caspase-9 is unaltered by UV treatment. *A,* MCF-7 cells were transfected with either empty vector (mock) or Bcl-2 as described under "Experimental Procedures" or not transfected (control). Forty-eight hours post-transfection apoptosis was induced by TNF-α (100 ng/ml) or UV irradiation (10 J/m²). Six hours later the cells were harvested, and the cell lysates were subjected to SDS-PAGE and Western blot analyses to determine the extent of caspase-7 cleavage and Bcl-2 expression. Western analysis of tubulin indicates similar protein loading in each lane. *B,* MCF-7 cells were plated and serum-starved. The following day cells were treated with UV irradiation (10 J/m²). At the times indicated, the cells were harvested and lysed. The lysates were immunoprecipitated with cross-linked anti-caspase-9 beads as described under "Experimental Procedures." Immunoprecipitation reactions (*top panel*) as well as 60 μg of whole cell lysates from the same samples (*bottom panel*) were then subjected to SDS-PAGE and Western blot analysis. Pro-caspase-9 Western analysis was used as a loading control for immunoprecipitations. *SFM,* serum-free medium.

caspase-9 may be altered with either IGF-I and/or UV treatment. Fig. 6*B* illustrates that XIAP was co-immunoprecipitated with a caspase-9 antibody, and its binding did not significantly change with either IGF-I or UV treatment at various time points. Western blot analyses of the same samples using whole cell lysates showed that cleaved caspase-9 and XIAP expression were also unchanged. In conclusion, we believe that the intrinsic pathway is inactive in MCF-7 cells, and this defect may be a result of an inhibitor of cytochrome *c* or the apoptosome.

UV Treatment Induces PARP and Caspase-8 Cleavage Independent of Caspase-9—Despite our results showing that the intrinsic pathway does not transmit an apoptotic signal in MCF-7 cells, our studies also confirm that MCF-7 cells can undergo UV-induced apoptosis. Typically, UV irradiation induces cells to undergo apoptosis via mitochondrial release of cytochrome *c* from the intermembrane space into the cytosol. Cytochrome *c* in the cytosol, in the presence of dATP, complexes with Apaf-1 and pro-caspase-9, resulting in caspase-9 autocatalytic activity. Although poorly characterized, other studies have suggested that caspase-8 could be indirectly involved in UV-mediated cell death by subsequent cytokine release and receptor activation or via a positive feedback loop subsequent to caspase-9 activation (31–33). In an effort to identify the caspase-9 independent pathway induced by UV irradiation, we asked whether UV could induce cleavage of the initiator caspase-8, which could then cleave caspase-7. As a positive control for caspase-8 activation, MCF-7 cells were treated for 4, 6, or 8 h with TNF-α and cycloheximide. As shown in Fig. 7, TNF-α induced activation of caspase-8 and PARP cleavage, indicating that the cells were undergoing apoptosis as expected. Interestingly, UV irradiation also activated caspase-8, although to a lesser extent than with TNF-α. PARP cleavage was also less robust with UV treatment at the dose used (10 J/m²). Again, caspase-9 cleavage was insensitive to
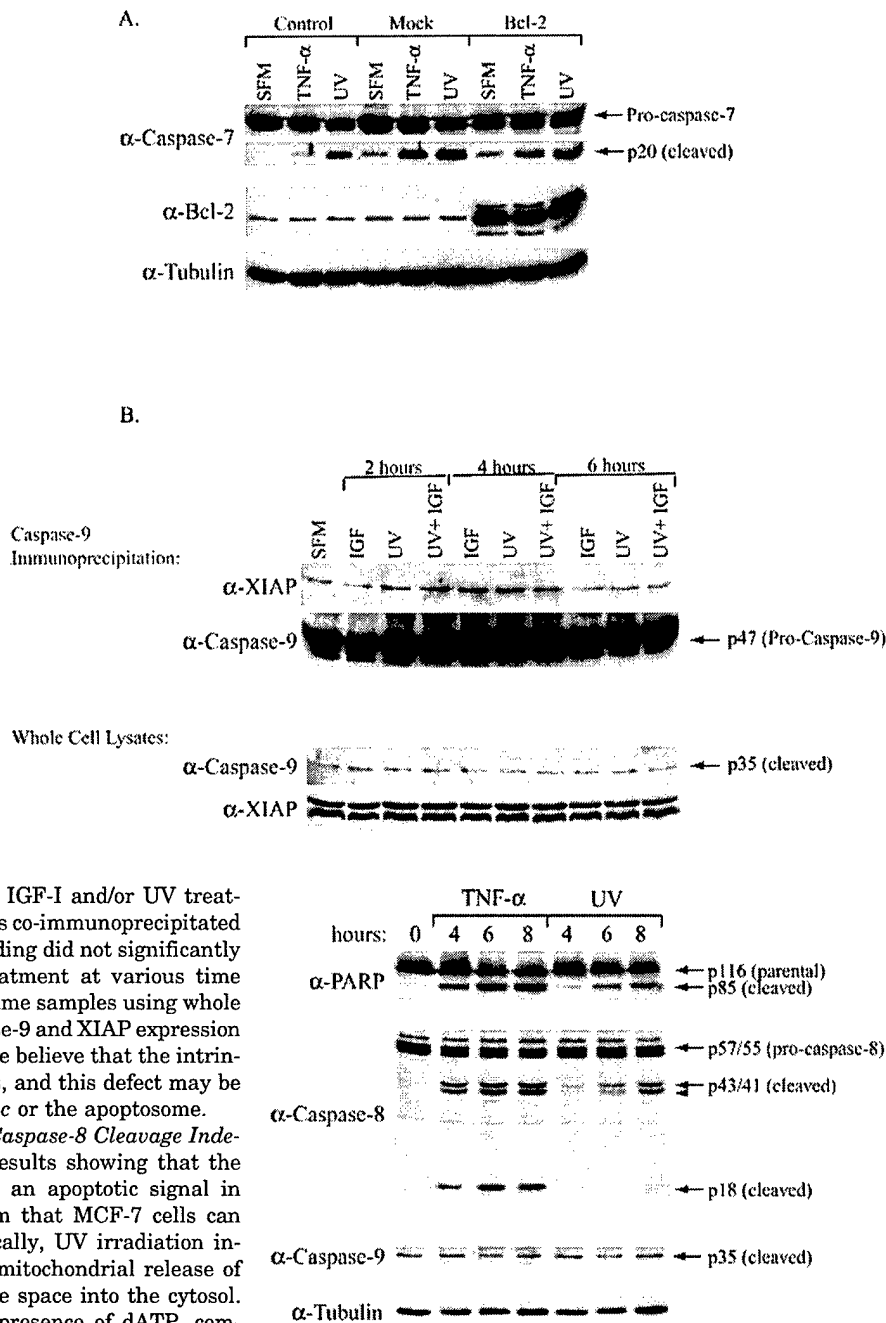

FIG. 7. TNF-α and UV treatment both result in caspase-8 and PARP cleavage, whereas caspase-9 cleavage is unchanged. To determine whether UV treatment can result in activation of the initiator caspase-8, MCF-7 cells were serum-starved for 18 h before treatment with either UV irradiation (10 J/m²) or TNF-α (100 ng/ml) and cycloheximide (1 μg/ml). At the times indicated, the cells were harvested. The cell lysates were subjected to SDS-PAGE and Western blot analyses to determine the extent of PARP, caspase-9, and caspase-8. Western analysis of tubulin indicates similar protein loading in each lane.

either treatment, indicating that apoptosis was occurring independently of caspase-9 and that pro-caspase-8 may be the initiator caspase with UV treatment. Because catalytically active caspase-8 is known to cleave the effector caspase-7, we conclude that UV-mediated apoptosis can occur independently of mitochondrial release of cytochrome *c* and subsequent activation of caspase-9 (5, 6).

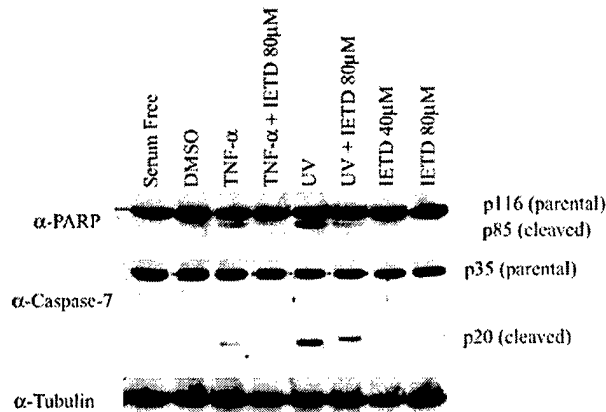To determine the role of caspase-8 in UV-induced apoptosis

FIG. 8. **Inhibition of caspase-8 by Z-IETD-FMK results in reduction of TNF-α- and UV-induced apoptosis.** To investigate the contribution of caspase-8 to apoptosis, MCF-7 cells were pretreated with 80 μM Z-IETD-FMK or Me₂SO (*DMSO*) only (vehicle control) for 30 min prior to treatment with TNF-α (100 ng/ml) or UV irradiation (10 J/m²). Six hours later the cells were harvested, and the cell lysates were subjected to SDS-PAGE and Western blot analyses to determine the extent of PARP and caspase-7 cleavage. Western analysis of tubulin indicates similar protein loading in each lane.

more directly, we took advantage of a commercially available cell-permeable caspase-8 inhibitor, Z-IETD-FMK. As shown in Fig. 8, treatment with Z-IETD-FMK dramatically reduced apoptosis following treatment with either TNF-α or UV irradiation in MCF-7 cells, as measured by PARP and pro-caspase-7 cleavage. Cleavage of pro-caspase-8 was unaffected with Z-IETD-FMK treatment, as expected, because the mechanism of action of the inhibitor is to block the active site of caspase-8 rather than inhibiting pro-caspase-8 processing (data not shown). These results demonstrate a critical role for caspase-8 in both TNF-α- and UV-induced apoptosis pathways in MCF-7 cells.

DISCUSSION

Under normal circumstances, apoptotic pathways are tightly regulated in organisms to assure appropriate growth and development. Clearly, aberrations of apoptosis have been documented in many diseases such as autoimmunity and cancer. In an effort to identify the underlying mechanisms of these diseases, executioners of apoptosis such as caspases, Smac/Diablo, and pro-apoptotic Bcl-2-related proteins have been described, along with proteins that inhibit apoptotic responses to cellular stress including IAPs and anti-apoptotic Bcl-2-related proteins. Much attention has focused on the function of caspase-9 and its requirement of the apoptosome for activity. Caspase-9 is of particular interest because it initiates cell death in response to non-cytokine-mediated cellular stress. The tightly regulated function of caspase-9 is crucial for development of the central nervous system; embryos of caspase-9 and Apaf-1 knockout mice show gross abnormalities in the brain and central nervous system (reviewed by Ranger *et al.* (34)).

In contrast, aberrations in mitochondrial apoptotic signals or caspase-9 function are better tolerated and more frequently observed in cancer cells resulting in treatment resistance (35). Because activated Akt phosphorylates pro-caspase-9 to inhibit its activity (13) and because caspase-9 is required downstream of p53 for p53-mediated apoptosis (25, 36), caspase-9 has become an important cancer target. Loss of p53 function or p53-mediated responses are both commonly observed in various forms of cancer; thus understanding the potential mechanisms of caspase-9 resistance to stress stimuli is of utmost importance in offsetting treatment resistance. To this end, significant progress has been made to identify the mechanisms for Bcl-2 or Bcl-XL-mediated cell survival and treatment resistance. One

mechanism for these effects is the ability of these proteins to inhibit mitochondrial membrane potential and cytochrome *c* release (15, 37), as well as their ability to bind and inhibit the activity of the apoptosome (14, 17, 18). Thus, overexpression of these proteins alters cellular response to stress at the level of the mitochondria and/or the apoptosome. Bcl-2 overexpression in MCF-7 cells had little effect after UV treatment, indicating either that the intrinsic pathway is not significantly contributing to the induction of apoptosis in these cells or that Bcl-2 is not inhibiting apoptosome function. IAPs can also inhibit apoptosis via binding to caspases-3, -7, and -9; the BIR3 domain of XIAP inhibits caspase-9 by direct binding to caspase-9 within the apoptosome (19, 20, 38). In our model, endogenous XIAP binding to caspase-9 did not significantly change with UV treatment. Because XIAP can also bind and inactivate caspase-7, we do not believe that role for XIAP is supported in this model because caspase-7 appears to be cleaving PARP in the absence of caspase-3. We show that in MCF-7 cells, other mechanisms of resistance must also exist that affect cytochrome *c* function. To our knowledge, this is the first report identifying an aberration in cytochrome *c* function after mitochondrial release, resulting in caspase-9 unresponsiveness.

Given the importance of cytochrome *c* in cell respiration and metabolism, one would expect that cells would not survive gross changes in protein structure or mitochondrial function. Indeed, we did not observe any alterations in the DNA sequence of cytochrome *c* derived from MCF-7 cells. Given that MCF-7 cells were able to respond to cellular stress by releasing mitochondrial cytochrome *c* but that only exogenous cytochrome *c* induced notable caspase-9 cleavage changes, we believe that our data are consistent with the presence of a cytoplasmic inhibitor of cytochrome *c*. In reviewing the literature to compare our findings, we note that many investigators have assessed pro-caspase-9 cleavage in MCF-7 cells using a cell-free system (4, 33) or microinjection of exogenous cytochrome *c*, concluding that MCF-7 cells are cytochrome *c*-insensitive (39). Typically, exogenous forms of pro-caspase-9, dATP, and cytochrome *c* are used in these reactions to detect caspase cleavage with high specificity and sensitivity, but they are not designed to test the function of endogenous caspase-9 or cytochrome *c*. Although microinjection of cytochrome *c* tests the function of endogenous proteins downstream of the mitochondria, it also does not ascertain endogenous cytochrome *c* function. Further, by adding exogenous cytochrome *c*, both assays may increase cytochrome *c* concentrations beyond that which any endogenous inhibitor can bind.

Other investigators report that caspase-9 transfection of MCF-7 cells induces apoptosis, independent of treatment (9, 40). We also have observed treatment-independent apoptosis with MCF-7 cells overexpressing pro-caspase-9 but only after reaching very high expression levels. In the studies described herein, we specifically expressed levels of caspase-9 that did not lead to apoptosis in the untreated transfectants to best mimic the *in vivo* functions of stress-induced caspase-9 activity. Finally, some groups have described treatment-induced cleavage of endogenous caspase-9 using MCF-7 cells (41). Such disparate results may occur from *in vitro* selection conditions because it is well accepted that the MCF-7 cell line may vary depending on *in vitro* culture conditions. We have confirmed our findings using MCF-7 cells from another source but are unable to study all sources. Despite these potential variations, we propose that MCF-7 cells offer a unique opportunity to study apoptotic mechanisms that occur independent of cytochrome *c*.

These considerations do not detract from the novelty of our findings, in that alterations in cytochrome *c* function have been

greatly overlooked to date, whereas other mechanisms of resistance to apoptosis have been rapidly advanced. Because cytochrome *c* is a necessary component of the apoptosome, its loss of function would have notable consequences to chemically induced apoptosis in most cells. Surprisingly, our findings with MCF-7 cells suggest that this may not be the case in our particular model. Our data are consistent with a cytochrome *c*-independent, caspase-dependent pathway conveying UV-mediated apoptosis. We propose that caspase-8 can function as the initiator caspase in these circumstances. MCF-7 cells neither express full-length caspase-3 to induce a positive feedback loop (33) nor appear to induce apoptosome formation *in vivo*. Further, caspase-2 cleavage was unchanged with UV treatment (data not shown). Thus, our data support that caspase-8 activation by UV treatment results in caspase-7 and PARP cleavage, without the requirement of tBid to induce cytochrome *c* translocation and pro-caspase-9 cleavage (see Ref. 42 for review).

We were also intrigued by the observation that MCF-7 cells harbor cleaved caspase-9 in an unstressed state. We propose two possible explanations for this observation. First, in the presence of a cytochrome *c* inhibitor, the level of cleaved pro-caspase-9 may be below the threshold necessary for induction of apoptosis, although with pro-caspase-9 transfection we observed significantly higher levels of cleavage product without any apparent changes in downstream caspase-7 or PARP. Another explanation may lie in the observations made by Alnemri and co-workers (4, 10) using an Apaf-1 mutant (Apaf-530) that lacks its WD-40 repeats and thus cannot bind cytochrome *c*. Experiments using this Apaf-1 mutant show that it oligomerizes and processes pro-caspase-9 in the absence of cytochrome *c* and dATP. However, processed caspase-9 is not released from the apoptosome. Although not directly comparable, these findings may explain why we observe some cleaved caspase-9 in unstressed MCF-7 cells that may have no effect on apoptosis if not released from the apoptosome. On the other hand, deletion of the WD-40 domain may simply result in the loss of an inhibitory function on Apaf-1 itself (4), suggesting that this mutant better describes the importance of the WD-40 domain on Apaf-1 structure than on the importance of cytochrome *c* binding. In fact, little is known structurally about how cytochrome *c* binds to Apaf-1 to form a functional apoptosome or the consequences of cytochrome *c* inhibition in this model. However, studies to identify the cytoplasmic, cytochrome *c* inhibitor and to characterize its biological function(s) are currently underway in our laboratory.

REFERENCES

1. Shi, Y. (2002) *Mol. Cell* **9**, 459–470
2. Wang, X. (2001) *Genes Dev.* **15**, 2922–2933
3. Zou, H., Li, Y., Liu, X., and Wang, X. (1999) *J. Biol. Chem.* **274**, 11549–11556
4. Srinivasula, S. M., Ahmad, M., Fernandes-Alnemri, T., and Alnemri, E. S. (1998) *Mol. Cell* **1**, 949–957
5. Srinivasula, S. M., Ahmad, M., Fernandes-Alnemri, T., Litwack, G., and Alnemri, E. S. (1996) *Proc. Natl. Acad. Sci. U. S. A.* **93**, 14486–14491
6. Muzio, M., Salvesen, G. S., and Dixit, V. (1997) *J. Biol. Chem.* **272**, 2952–2956
7. Li, H., Zhu, H., Xu, C., and Yuan, J. (1998) *Cell* **94**, 491–495
8. Hakem, R., Hakem, A., Dunscan, G. S., Henderson, J. T., Woo, M., Soengas, M. S., Elia, A., de la Pompa, J. L., Kagi, D., Khoo, W., Potter, J., Yoshida, R., Kaufman, S. A., Lowe, S. W., Penninger, J. M., and Mak, T. W. (1998) *Cell* **94**, 339–352
9. Li, P., Nijhawan, D., Budihardjo, I., Srinivasula, S. M., Ahmad, M., Alnemri, E. S., and Wang, X. (1997) *Cell* **91**, 479–489
10. Saleh, A., Srinivasula, S., Acharya, S., Fishel, R., and Alnemri, E. S. (1999) *J. Biol. Chem.* **274**, 17941–17945
11. Lassus, P., Rodriguez, J., and Lazebnik, Y. (2002) *Science* **297**, 1352–1354
12. Cain, K., Brown, D. G., Langlais, C., and Cohen, G. M. (1999) *J. Biol. Chem.* **274**, 22686–22692
13. Cardone, M. H., Roy, N., Stennicke, H. R., Salvesen, G. S., Franke, T. F., Stanbridge, E., Frisch, S., and Reed, J. C. (1998) *Science* **282**, 1318–1321
14. Kharbanda, S., Pandey, P., Schofield, L., Israels, S., Roncinske, R., Yoshida, K., Bharti, A., Yuan, Z. M., Saxena, S., Weichselbaum, R., Nalin, C., and Kufe, D. (1997) *Proc. Natl. Acad. Sci. U. S. A.* **94**, 6939–6942
15. Kluck, R. M., Bossy-Wetzel, E., Green, D. R., and Newmeyer, D. D. (1997) *Science* **275**, 1132–1136
16. Yang, J., Liu, X., Bhalla, K., Kim, C. N., Ibrado, A. M., Cai, J., Peng, T.-I., Jones, D. P., and Wang, X. (1997) *Science* **275**, 1129–1132
17. Hu, Y., Benedict, M. A., Wu, D., Inohara, N., and Nunez, G. (1998) *Proc. Natl. Acad. Sci. U. S. A.* **95**, 4386–4391
18. Pan, G., O'Rourke, K., and Dixit, V. M. (1998) *J. Biol. Chem.* **273**, 5841–5845
19. Deveraux, Q. L., Roy, N., Stennicke, H. R., Van Arsdale, T., Zhou, Q., Srinivasula, S. M., Alnemri, E. S., Salvesen, G. S., and Reed, J. C. (1998) *EMBO J.* **17**, 2215–2223
20. Deveraux, Q. L., Leo, E., Stennicke, H. R., Welsh, K., Salvesen, G. S., and Reed, J. C. (1999) *EMBO J.* **18**, 5242–5250
21. Verhagen, A. M., Ekert, P. G., Pakusch, M., Silke, J., Connolly, L. M., Reid, G. E., Moritz, R. L., Simpson, R. J., and Vaux, D. L. (2000) *Cell* **102**, 43–53
22. Du, C., Fang, M., Li, Y., Li, L., and Wang, X. (2000) *Cell* **102**, 33–42
23. Soengas, M. S., Capodicci, P., Polsky, D., Mora, J., Esteller, M., Opitz-Araya, X., McCombie, R., Herman, J. G., Gerald, W. L., Lazebnik, Y. A., Cardon-Cardo, C., and Lowe, S. W. (2001) *Nature* **409**, 207–211
24. Wolf, B. B., Schuler, M., Li, W., Eggers-Sedlet, B., Lee, W., Tailor, P., Fitzgerald, P., Mills, G. B., and Green, D. R. (2001) *J. Biol. Chem.* **276**, 34244–34251
25. Soengas, M. S., Larcon, R. M., Yoshida, H., Giaccia, A. J., Hakem, R., Mak, T., and Lowe, S. W. (1999) *Science* **284**, 156–159
26. Janicke, R. U., Sprengart, M. L., Wati, M. R., and Porter, A. G. (1998) *J. Biol. Chem.* **273**, 9357–9360
27. Blanc, C., Deveraux, Q. L., Krajewski, S., Janicke, R. U., Porter, A. G., Reed, J. C., Jaggi, R., and Marti, A. (2000) *Cancer Res.* **60**, 4385–4390
28. Germain, M., Affar, E. B., D'Amours, D., Dixit, V. M., Salvesen, G. S., and Poirier, G. G. (1999) *J. Biol. Chem.* **274**, 28379–28384
29. Bratton, S. B., Walker, G., Srinivasula, S. M., Sun, X. M., Butterworth, M., Alnemri, E. S., and Cohen, G. M. (2001) *EMBO J.* **20**, 998–1009
30. Fang, G., Chang, B. S., Kim, C. N., Perkins, C., Thompson, C. B., and Bhalla, K. N. (1998) *Cancer Res.* **58**, 3202–3208
31. Sun, X.-M., MacFarlane, M., Zhuang, J., Wolf, B. B., Green, D. R., and Cohen, G. M. (1999) *J. Biol. Chem.* **274**, 5053–5060
32. Tang, D., Lahti, J. M., and Kidd, V. J. (2000) *J. Biol. Chem.* **275**, 9303–9307
33. Slee, E. A., Harte, M. T., Kluck, R. M., Wolf, B. B., Casiano, C. A., Newmeyer, D. D., Wang, H.-G., Reed, J. C., Nicholson, D. W., Alnemri, E. S., Green, D. R., and Martin, S. J. (1999) *J. Cell Biol.* **144**, 281–292
34. Ranger, A. M., Malynn, B. A., and Korsmeyer, S. J. (2001) *Nat. Genet* **28**, 113–118
35. Debatin, K. M., Poncet, D., and Kroemer, G. (2002) *Oncogene* **21**, 8786–8803
36. Sabbatini, P., and McCormick, F. (1999) *J. Biol. Chem.* **274**, 24263–24269
37. Stegh, A. H., Barnhart, B. C., Volkand, J., Algeciras-Schimnich, A., Ke, N., Reed, J. C., and Peter, M. (2002) *J. Biol. Chem.* **277**, 4351–4330
38. Srinivasan, S. M., Hegde, R., Saleh, A., Datta, P., Shiozaki, E., Chal, J., Lee, R.-A., Robbins, P. D., Fernandes-Alnemri, T., Shi, Y., and Alnemri, E. S. (2001) *Nature* **410**, 112–116
39. Li, F., Srinivasan, A., Wang, Y., Armstrong, R. C., Tomaselli, K. J., and Fritz, L. C. (1997) *J. Biol. Chem.* **272**, 30299–30305
40. Duan, H., Orth, K., Chinnaiyan, A. M., Poirier, G. G., Froelich, C. J., He, W. W., and Dixit, V. M. (1996) *J. Biol. Chem.* **271**, 16720–16724
41. Niu, M.-Y., Menard, M., Reed, J. C., Krajewska, S., and Pratt, M. A. C. (2001) *Oncogene* **20**, 3506–3518
42. Van Loo, G., Saelens, X., Van Gurp, M., MacFarlane, M., Martin, S. J., and Vandenabeele, P. (2002) *Cell Death Differ.* **9**, 1031–1042

An inhibitory function for JNK in the regulation of IGF-I signaling in breast cancer

Cindy L Mamay[1], Amy M Mingo-Sion[2], Doug M Wolf[2,3], Marion D Molina[2] and Carla L Van Den Berg*[,2]

[1]Department of Biological Chemistry, University of California, Davis, CA 95616-8655, USA; [2]School of Pharmacy, University of Colorado Health Sciences Center, 4200 East Ninth Avenue, Campus Box C238, Denver, CO 80262, USA; [3]Department of Obstetrics and Gynecology, School of Medicine, University of Colorado Health Sciences Center, 4200 East Ninth Avenue, Campus Box B198, Denver, CO 80262, USA

Insulin-like growth factor-I receptor (IGF-IR) is frequently overexpressed in a variety of cancer types. Since many breast tumors and cancer cell lines overexpress IGF-IR, we tested IGF-I effects on chemotherapy-treated breast cancer cells. IGF-I protects from chemotherapy-induced apoptosis, suggesting that overlapping signaling pathways modulate IGF-I and chemotherapy treatment outcomes. Taxol and other chemotherapy drugs induce c-Jun N-terminal kinase (JNK), a kinase that conveys cellular stress and death signals. Notably, in this paper we show that IGF-I alone induces a potent JNK response and this activity is reversed by inhibition of phosphatidylinositol 3-kinase (PI 3-kinase) with LY294002 in MCF-7 but not T47D cells. Cotreatment of cells with chemotherapy and IGF-I leads to additive JNK responses. Using cells overexpressing Akt, we confirm that IGF-I-mediated survival is Akt dependent. In contrast, overexpression of JNK significantly enhances Taxol-induced apoptosis and inhibits IGF-I survival effects. Further, JNK attenuates anchorage-independent growth of MCF-7 cells. The inhibitory effect of JNK appears to be mediated by serine phosphorylation of IRS-1 (insulin receptor substrate) since both Taxol and IGF-I treatment enhanced Ser^{312} IRS-1 phosphorylation, while LY294002 blocked IGF-I-mediated phosphorylation. Taken together, these data provide a mechanism whereby stress or growth factors activate JNK to reduce proliferation and/or survival in breast cancer cells.
Oncogene (2003) **22**, 602–614. doi:10.1038/sj.onc.1206186

Keywords: IGF-I; JNK; IRS-1; breast cancer; apoptosis

Introduction

The importance of insulin-like growth factor-I receptor (IGF-IR) action in breast cancer has been clearly demonstrated. Its expression has been observed in 87% of breast cancer specimens (Peyrat *et al.*, 1990),

*Correspondence: CL Van Den Berg;
E-mail: carla.vandenberg@UCHSC.edu

and overexpressed IGF-IR in human tumor specimens is functional, having increased kinase activity compared to normal mammary tissue (Resnik *et al.*, 1998). Furthermore, Cullen and colleagues (Cullen *et al.*, 1990; Singer *et al.*, 1995) have shown that breast cancer evolution is associated with the induction of IGF-II secretion, another IGF-IR ligand, from stromal cells neighboring malignant breast tissue. Butler *et al.* (1998) have shown that systemically administered IGF-I stimulates tumor growth in mice in a dose-dependent fashion using NIH 3T3 cells overexpressing IGF-IR. Inhibition of IGF-IR activity by overexpression of a dominant-negative form of IGF-IR in MDA-MB-231 and MDA-MB-435 breast cancer cell lines inhibits the adhesion, invasion, and metastasis of these cells, as well as enhances their sensitivity to Taxol-induced cell death (Dunn *et al.*, 1998). Some of these IGF-IR-mediated tumorigenic properties may be attributed to its central role in the regulation of proteins important for either matrix attachment or cell survival.

Activated IGF-IR imparts both survival and proliferative effects in various experimental models including neuronal and cancer cells. After IGF-IR autophosphorylation, IGF-IR complexes with and tyrosine phosphorylates IRS docking proteins which then activate second messengers, such as mitogen-activated protein kinase (MAPK), also known as extracellular signal-related kinase (ERK) and PI 3-kinase. Recently, many significant observations have been published regarding the role of serine/threonine kinases that phosphorylate IRS-1. Interestingly, serine phosphorylation of IRS-1 by downstream kinases can regulate IRS-1 tyrosine phosphorylation status and its ability to serve as a substrate to insulin receptor (IR) or IGF-IR. Based on IRS-1's sequence, there are 35 potential serine/threonine phosphorylation sites. Some of these sites, when phosphorylated, result in either sustained or abbreviated IRS tyrosine phosphorylation, modifying downstream responses in a positive or negative fashion. Activation of pathways involving PI 3-kinase, Akt, GSK3 (glycogen synthase kinase-3), MAPK, and c-Jun N-terminal kinase (JNK) (among others) is known to serine phosphorylate various IRS-1 sites and presumably the duration of IGF-I or insulin signaling. Further,

IRS-1 signaling may be mediated by proteasome degradation subsequent to ligand binding; this activity is also mediated through PI 3-kinase but not MAPK (Lee et al., 2000).

Soon after PI 3-kinase activity is enhanced by binding to IRS-1, activation of downstream kinases Akt and/or p70 S6 kinase occurs. PI 3-kinase activation of Akt conveys many growth-factor-dependent survival effects (Kennedy et al., 1997). Enhanced Akt activity results in inhibition of many cell death proteins through phosphorylation of BAD (BCL-X_L/BCL-2 associated death promoter) (Datta et al., 1997), the protease caspase-9 (Cardone et al., 1998), and the forkhead transcription factor family (Brunet et al., 1999).

In addition to inducing PI 3-kinase-dependent responses, IGF-I also strongly activates MAPK in MCF-7 and T47D breast cancer cells. MAPK inhibition by the pharmacologic agent PD0908059 reduces proliferation of MCF-7 and T47D cells, thus implicating a role for MAPK in IGF-I-mediated proliferation (Hermanto et al., 2000). Another MAPK family protein that is also activated by IGF-I is JNK (Monno et al., 2000); however, the function of this activation is poorly understood. In fact, others have shown that IGF-I pretreatment inhibits JNK activity induced by tumor necrosis factor-α (TNFα), and anisomycin in 293 cells (Okubo et al., 1998). Since JNK is activated by diverse cell stimuli, including stress, growth factors (i.e. epidermal growth factor (EGF)), and cytokines (i.e. TNFα and interleukin-1) (Sluss et al., 1994; Whitmarsh et al., 1995; Rosette and Karin, 1996), JNK-mediated effects can be proapoptotic, proliferative, or antiproliferative.

JNK is best characterized by its sensitivity to stress treatments like anisomycin, irradiation, and TNFα. Many chemotherapy drugs also induce JNK as a result of DNA damage or microtubule interference. In particular, microtubule-interfering agents (MIAs), such as paclitaxel (Taxol) and docetaxel (Taxotere), activate JNK through pathways involving Ras and ASK1 apoptosis signal-regulating kinase-1 (Chen et al., 1996; Wang et al., 1998), indicating that activation of JNK is needed to initiate the microtubular disarray caused by MIAs. Thus, there is considerable evidence to support the role of JNK in regulating apoptosis following cellular stress. When JNK activity is enhanced by chemotherapeutic agents and radiation, it signals cells to undergo programmed cell death (Chen et al., 1996; Wang et al., 1998).

In this study, we investigated the mechanism(s) of IGF-I survival responses in chemotherapy-treated breast cancer cells. We focused on JNK activation by the MIA, Taxol, and sought to determine if this activation might be altered by IGF-I cotreatment in breast cancer cells. We initially hypothesized that IGF-IR chemoprotective effects in our model result from stimulation of PI 3-kinase and its downstream effector, Akt. Here, we confirm that Akt has a significant role in IGF-I-mediated survival; however, we also show that IGF-I treatment alone potently activates JNK in breast cancer cell lines. In MCF-7 cells, but not in T47D cells, this action is significantly reduced by PI 3-kinase

inhibition. Cotreatment of breast cancer cells with Taxol and IGF-I results in an additive increase in JNK activity. The resulting cellular outcome of JNK over-expression is attenuation of IGF-I responses. These inhibitory effects of JNK on IGF-I responses appear to result from phosphorylation of human Ser[312] (corresponding to rat Ser[307]) on IRS-1. Altogether, these results suggest that IGF-I may downregulate its own survival effects via activation of JNK, thus abrogating its ability to promote cell survival or proliferation.

Materials and methods

Cell culture and treatments

MCF-7 cells were provided by C Kent Osborne (San Antonio, TX, USA) and T47D cells were obtained from the University of Colorado Cancer Center, Tissue Culture Core (Denver, CO, USA). Both cell lines were maintained in full media improved minimal essential medium (IMEM) with phenol red (Mediatech, Herndon, VA, USA) supplemented with 10% fetal bovine serum (Gemini, Calabasas, CA, USA), antibiotics, glutamine, and insulin. In each experiment, cells were plated in full media and cultured overnight at 37°C and 5% CO_2. The following day, cells were washed twice with warm phosphate-buffered saline (PBS, Biofluids, Rockville, MD, USA) and then cultured overnight in serum-free media (SFM). The next day, cells were treated with IGF-I (Bioreclamation, Hicksville, NY, USA and the National Hormone and Pituitary Program obtained from NHPP, NIDDK and Dr AF Parlow), Taxol (paclitaxel (Mead Johnson, Princeton, NJ, USA)), or Taxotere (docetaxel (Rhone-Poulenc Rorer Pharmaceuticals, Collegeville, PA, USA)) as described in figure legends. Pretreatments with either 100 nM wortmannin or 50–100 μM LY294002 as indicated (Calbiochem and Alexis Biochemicals, respectively, San Diego, CA, USA) were performed 40 min prior to stimulation with IGF-I. All protein concentrations from cell extracts were determined using a Bio-Rad D/C protein assay kit (Bio-Rad, Hercules, CA, USA).

Transfection experiments

Hemagglutinin (HA)-tagged Akt and Akt (K179A, kinase dead) vectors were graciously provided by ME Greenberg (Datta et al., 1997). The myr-HA-Akt pcDNA3 construct was a gift from JR Testa (Mitsuuchi et al., 2000). JNK and JNK (T183A/Y185F, kinase dead) pcDNA3 constructs were obtained from C Franklin, University of Colorado Health Sciences Center. Generation of both wild-type (Wt) and mutant (Mt) Akt and JNK stable transfectants was performed by plating 2×10^6 of MCF-7 cells per 10 cm dish. The following day, cells were transfected with 10 μg of DNA by lipofection (Lipofectamine™, Gibco BRL, Grand Island, NY, USA). Control cells were transfected with empty vector. After 24–48 h, cells were selected with 800 μg/ml of G418. Individual resistant colonies were isolated and expanded. Detection of clones overexpressing either Akt and JNK Wt or Mt genes was performed by Western blot analysis using HA-probe (F-7) primary antibody (sc-7392, Santa Cruz Biotechnology, Santa Cruz, CA, USA). For transient transfections, 1.8×10^6 MCF-7 cells were plated in 60 mm dishes. The next day, cells were transfected using Lipofectamine™ and Plus™ reagent according to product(s) instructions (Gibco BRL, Grand Island, NY, USA). Cells were then placed in SFM overnight prior to treatment.

JNK assay and Western blot analysis

As a positive control for JNK activation, cells were plated and serum-starved as described previously. UV irradiation was performed by exposing cells to UVC (ultraviolet-C, $50 \, \text{J/m}^2$) in a Stratagene UV linker 1800 (Stratagene, La Jolla, CA, USA). Cells were then incubated at 37°C in 5% CO_2 for 50 min before preparing cell lysates. Other cells were plated and serum-starved and then exposed to either IGF-I and/or chemotherapy as indicated. Tissue culture dishes were washed twice with ice-cold PBS. Cells were harvested and *in vitro* kinase assays were performed as described previously (Hibi *et al.*, 1993) using cell lysate volumes corresponding to 400–600 μg of total protein. The products were then resolved by 10% SDS–PAGE (polyacrylamide gel electrophoresis). The gel was dried and subjected to radiography. Additionally, phosphorylated c-jun product incorporating ^{32}P was quantitated by PhosphorImager analysis.

To assure that kinase reactions in each experiment contained approximately equal amounts of JNK protein per sample, 10 μl of supernatant from each kinase reaction was run on a 10% SDS–PAGE. Proteins were transferred to Immobilon-P transfer membrane (Millipore, Bedford, MA, USA) and JNK protein quantity was verified by immunoblotting with JNK1 antibody (FL, Santa Cruz Biotechnology, Santa Cruz, CA, USA) and enhanced chemiluminescence (Amersham, Piscataway, NJ, USA).

Akt substrate construct, affinity purification, immobilized and soluble GST thrombin-Akt substrate

The peptide RPRAATF, corresponding to the sequence containing the threonine phosphorylation site of GSK-3, was fused in frame with GST in pGEX-4T-1 by first hybridizing the oligonucleotides (5′-AATTGCGTCCGCGTGCTGCCACC-TTCG-3′) and (5′-AATTCGAAGGTGGCAGCACGCGGA-CGC-3′) to produce a double-stranded DNA with *Eco*RI sticky ends. This DNA fragment was then cloned into the *Eco*RI site of pGEX-4T-1 (Pharmacia Biotech, Piscataway, NJ, USA), regenerating only one *Eco*RI site. A construct with the insert in the correct orientation was identified by restriction analysis and sequencing (University of Colorado Cancer Center DNA Sequencing Core Service). Affinity purification of the GST thrombin–Akt substrate fusion protein was performed as described by Smith and Johnson (1988).

Akt assay

After IGF-I treatment, tissue culture dishes were washed twice with ice-cold PBS. Cells were harvested in lysis buffer and kinase assays performed, as previously described (Franke *et al.*, 1995), using volumes of precleared lysate containing 400 μg of total protein for each sample. Reactions were terminated with 15 μl of 4 × sample buffer. The products were then resolved by 10% SDS–PAGE. The gel was dried and subjected to radiography. Additionally, phosphorylated product incorporating ^{32}P was quantitated by PhosphorImager analysis. Immunoprecipitation or Western blot analysis of Akt1 was performed using anti-Akt1 antibody (C20, Santa Cruz Biotechnology, Santa Cruz, CA, USA).

Apoptosis assays

A total of 75 000 MCF-7 cells were plated in each $1.7 \, \text{cm}^2$ chamber of Biocoat CultureSlides™ (Falcon, Becton Dickinson Labware, Franklin Lakes, NJ, USA). Cells were cultured overnight as described above. The following day, cells were washed twice with PBS and then exposed to SFM control,

IGF-I 50 ng/ml alone, Taxol 0.02 μM alone, or Taxol plus IGF-I as described in figure legends. At 48 h after exposure to treatment cells were fixed in 3% formaldehyde in PBS for 5 min, washed three times with PBS, and nuclei were stained with a solution containing 15 μM Hoechst 33258 in PBS for 10 min. A minimum of 200 cells were counted per treatment and the nuclei morphology determined as viable or apoptotic using a fluorescence microscope (Zeiss, Oberkochen, Germany).

Poly(ADP) ribose polymerase (PARP) cleavage was measured in cells transiently transfected (see above) with myr-HA-Akt-pcDNA3 or empty pcDNA3 vector. Additionally, PARP experiments using overexpressed JNK were from the stably transfected MCF-7 cells. Cells were treated as described above and lysed using EB buffer (20 mM Tris-HCl, pH 7.6, 0.25 M NaCl, 3 mM EDTA, 0.5% IGEPAL CA-630 with freshly added 1 mM DTT (dithiothreitol), 1 mM phenylmethylsulfonyl fluoride (PMSF), 20 μg/ml aprotinin, 5 μg/ml leupeptin, and 2 mM Na orthovanadate). A total of 70 μg of protein was then resolved by 10% SDS–PAGE. Proteins were transferred to nitrocellulose and Western blots performed using anti-PARP antibody (H250, sc-7150, Santa Cruz Biotechnology, Santa Cruz, CA, USA).

Anchorage-independent growth assays (AIG)

Parental MCF-7 or MCF-7 stable transfectants of Wt or Mt JNK were suspended in 5% charcoal stripped serum (css) (± IGF-I) and 0.4% SeaPlaque agarose (BioWhittaker Molecular Applications, East Rutherford, NJ, USA) at a density of 15×10^3 cells/35 mm dish. Cell suspensions were overlayed on a solidified bottom layer of 5% CSS and 0.6% SeaPlaque agarose and then incubated for 10 days at 37°C. Each group was assayed in triplicate dishes. On day 10, colonies equaling approximately ⩾ 20 cells were counted.

IRS-1 immunoprecipitation and Western blot analysis

Nontransfected and transfected cells were treated with IGF-I (50 ng/ml) and/or LY294006 (50 μM) according to figure legends. Cells were transfected with either empty vector or pEBG-JNK1 (a gift from Dr Kyriakis, Harvard University) according to the method described above. Following culture and/or transfection, cells were serum-starved overnight prior to treatment. Following treatment, cell lysates containing 300 μg of protein were incubated with 2.4 μg of anti-IRS-1 antibody (Upstate Biotechnology, Lake Placid, NY, USA) and 30 μg of rProtein G Agarose beads (Gibco, Gaithersburg, MD, USA) overnight at 4°C. Beads were washed three times in lysis buffer and resuspended in sample buffer. Samples were loaded on a 7% SDS–PAGE acrylamide gel, then transferred to nitrocellulose. Membranes were blocked in 5% milk in TBST, then incubated with either antiphospho-IRS-1(Ser[307]) (Upstate Biotechnology, Lake Placid, NY, USA) or an antiphosphotyrosine antibody (RC20, BD Transduction, San Diego, CA, USA). All Western blots were analysed using enhanced chemiluminescence according to the manufacturer's instructions (Amersham, Piscataway, NJ, USA).

Data analysis

Apoptosis assays were analysed by multiple logistic regression performed using SAS/PROC GENMOD, version 6.12 (SAS Institute, Carey, NC, USA). Tests were performed for overall effect of IGF-I or the transfected gene on Taxol-induced apoptosis, as well as for significant interaction effects between IGF-I and the transfected gene. As multiple comparisons were

JNK inhibits IGF-I function in breast cancer cells
CL Mamay et al
605

required to address all questions of interest, results were not considered statistically significant unless the contrast reached $P < 0.005$.

Results

MIA treatment activates JNK in breast cancer cells

The various biological outcomes of IGF-I treatment of breast cancer cells have been well described. However, less is known about the signaling pathways that allow IGF-I to convey its cytoprotective effects in chemotherapy-treated cancer cells. We initially set out to measure JNK response to chemotherapy in our model, and then to determine if IGF-I treatment might suppress stress-related signaling as a possible mechanism for its inhibition of programmed cell death. JNK activation in response to chemotherapy treatment has been suggested to correspond to cell sensitivity to chemotherapy (Potapova et al., 1995). Therefore, we tested if the chemotherapeutic agents, doxorubicin, Taxol, and Taxotere, induce JNK activity in MCF-7 breast cancer cells. Treated cells were harvested at various time points to determine the peak time of activation. Figure 1 illustrates that Taxol and Taxotere treatment of cells induced JNK activity approximately threefold, while JNK activation by doxorubicin is somewhat less than threefold. A bimodal pattern of JNK activation was observed with Taxol treatment, with early activation

occurring at 2 h of exposure and maximal activation observed at 8 h. Taxotere treatment led to similar levels of JNK induction as Taxol ($\geqslant$ threefold over control), however only one peak activation time occurred at 2 h of exposure.

IGF-I induces JNK via PI 3-kinase in MCF-7 cells

In order to study IGF-I's ability to regulate JNK in breast cancer cells, we measured the effect of IGF-I treatment alone on JNK activity. Initially, we predicted that IGF-I treatment alone would either (1) suppress JNK signaling, since many treatments that stimulate JNK result in cell death and IGF-I opposes this response or (2) have minimal effect on JNK, as other investigators have shown that tyrosine kinase receptor activation leads to low levels of JNK activity, generally peaking within 30 min of exposure (Kyriakas et al., 1994; Westwick et al., 1994; Fanger et al., 1997; Goedert et al., 1997; Alblas et al., 1998). Figure 2 shows that IGF-I potently stimulates JNK in both MCF-7 and T47D breast cancer cells. Maximal JNK activity was observed in MCF-7 cells after 2 h of exposure, when approximately a ninefold level of induction was typically observed in multiple experiments with MCF-7 cells; this JNK induction was notably more robust activation than what we observed with the chemotherapy agents. In T47D cells (Figure 2), JNK activation peaked at 30 min and was somewhat less than that observed in MCF-7 cells.
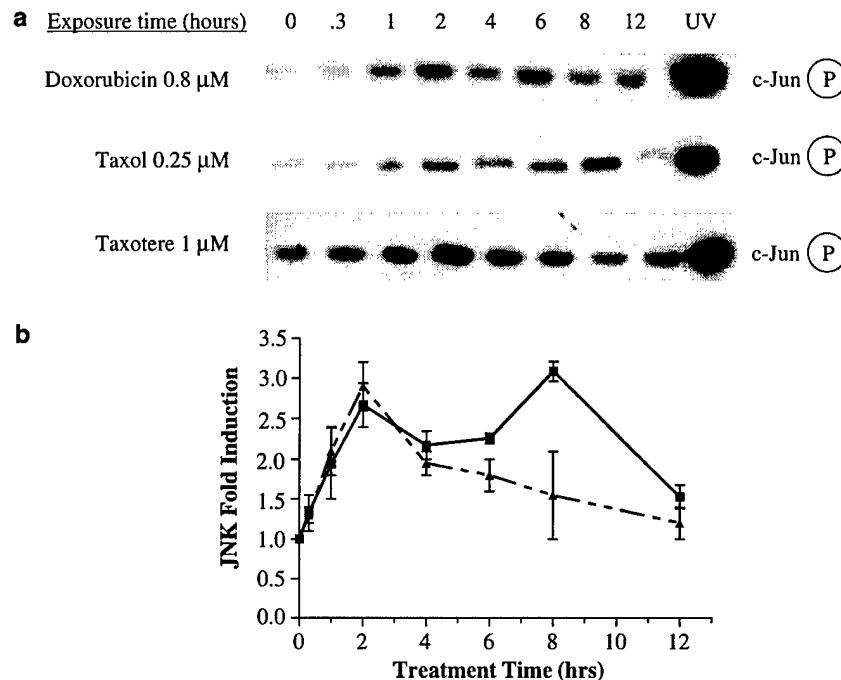

Figure 1 Taxol and Taxotere treatment increases JNK activity. (a) MCF-7 cells were treated with either doxorubicin (not shown graphically), Taxol (■), or Taxotere (▲) at concentrations indicated and harvested in a time-dependent fashion. UV (50 J/M²) was used as a positive control for JNK activation in MCF-7 cells. Analyses of phosphorylated c-Jun$_{(1-79)}$ resulting from in vitro kinase assays are shown. (b) The graph shows the combined results of two independent experiments (points: mean; bars: range)

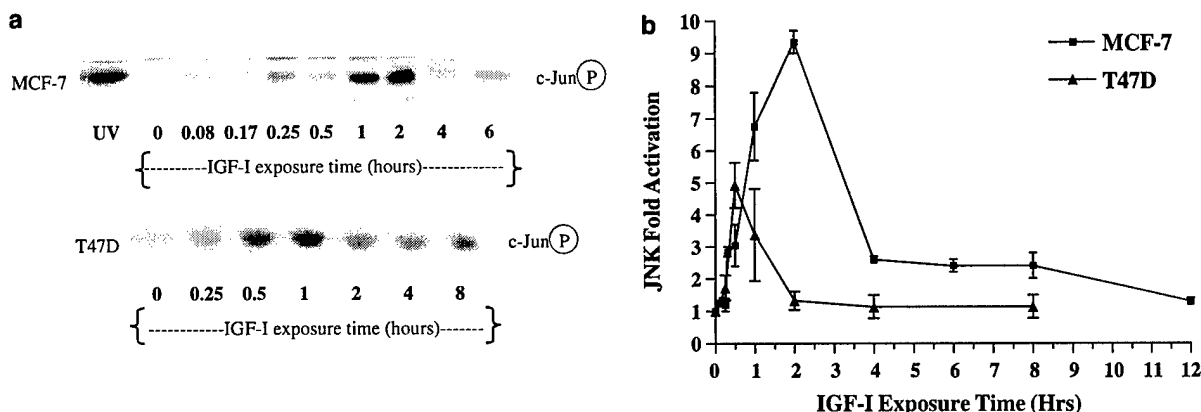**Figure 2** JNK activity is dramatically increased with IGF-I treatment in MCF-7 cells. MCF-7 and T47D breast cancer cells were treated with IGF-I (50 ng/ml) in a time-course experiment. (a) Analyses of phosphorylated c-Jun$_{(1-79)}$ resulting from *in vitro* kinase assays of MCF-7 cells are shown. UV (50 J/M^2) was used as a positive control for JNK activation in MCF-7 cells. (b) The graph shows the combined results of at least two independent experiments (mean±range)
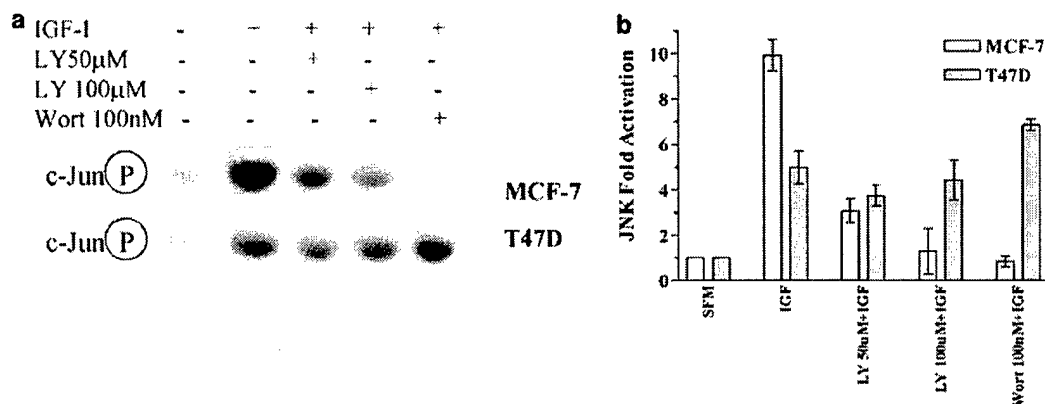

Figure 3 JNK activation by IGF-I is PI 3-kinase dependent in MCF-7 cells. (a) T47D and MCF-7 breast cancer cells were pretreated with LY294002 or wortmannin as indicated for 40 min prior to IGF-I treatment for 30 and 60 min, respectively. Analyses of phosphorylated c-Jun$_{(1-79)}$ resulting from *in vitro* kinase assays are shown. (b) The graph shows the combined results of at least two independent experiments (mean±range)

Since PI 3-kinase is a known second messenger for IGF-IR signaling, we sought to then determine if IGF-I activation of JNK is PI 3-kinase dependent. Addition of the PI 3-kinase inhibitors, wortmannin and LY294002, to IGF-I-treated MCF-7 cells significantly reduced IGF-I-dependent activation of JNK (Figure 3). Although IGF-I induced JNK activity in both breast cancer cell lines, use of both PI 3-kinase inhibitors showed that IGF-I activation of JNK was PI 3-kinase dependent in MCF-7 cells but not in T47D cells (Figure 3). These data support the hypothesis that PI 3-kinase lies upstream of JNK in MCF-7 cells treated with IGF-I and suggest that IGF-I activation of JNK through PI 3-kinase may influence IGF-I and/or Akt survival responses.

Combined IGF-I and MIA treatment results in an additive JNK response

We then assessed endogenous JNK response to cotreatment using IGF-I and chemotherapy to determine if these two treatments might counteract one another's signaling through JNK. UV treatment was also studied in cotreatment of cells to ascertain if IGF-I effects on JNK agonists could be extended to other stress treatments. MCF-7 cells were pretreated with either Taxol (for 5–7 h) or Taxotere (for 1 h), then IGF-I was added for the last hour of exposure, in order to harvest cells at the approximate times of maximal activity for each treatment. Figure 4a and b shows JNK phosphorylation of c-Jun substrate under the conditions described above. In contrast to a previous report (Okubo *et al.*, 1998) and our predictions, IGF-I cotreatment of cells did not interfere with JNK activation by other JNK-activating agents. In fact, JNK induction was higher with cotreatment when IGF-I was added after stress treatment (Figure 4) or simultaneously (data not shown). The greatest JNK activity was observed when cells were treated for the duration of time seen for maximal activity with each treatment alone. These conclusions can be extended to other stress treatments
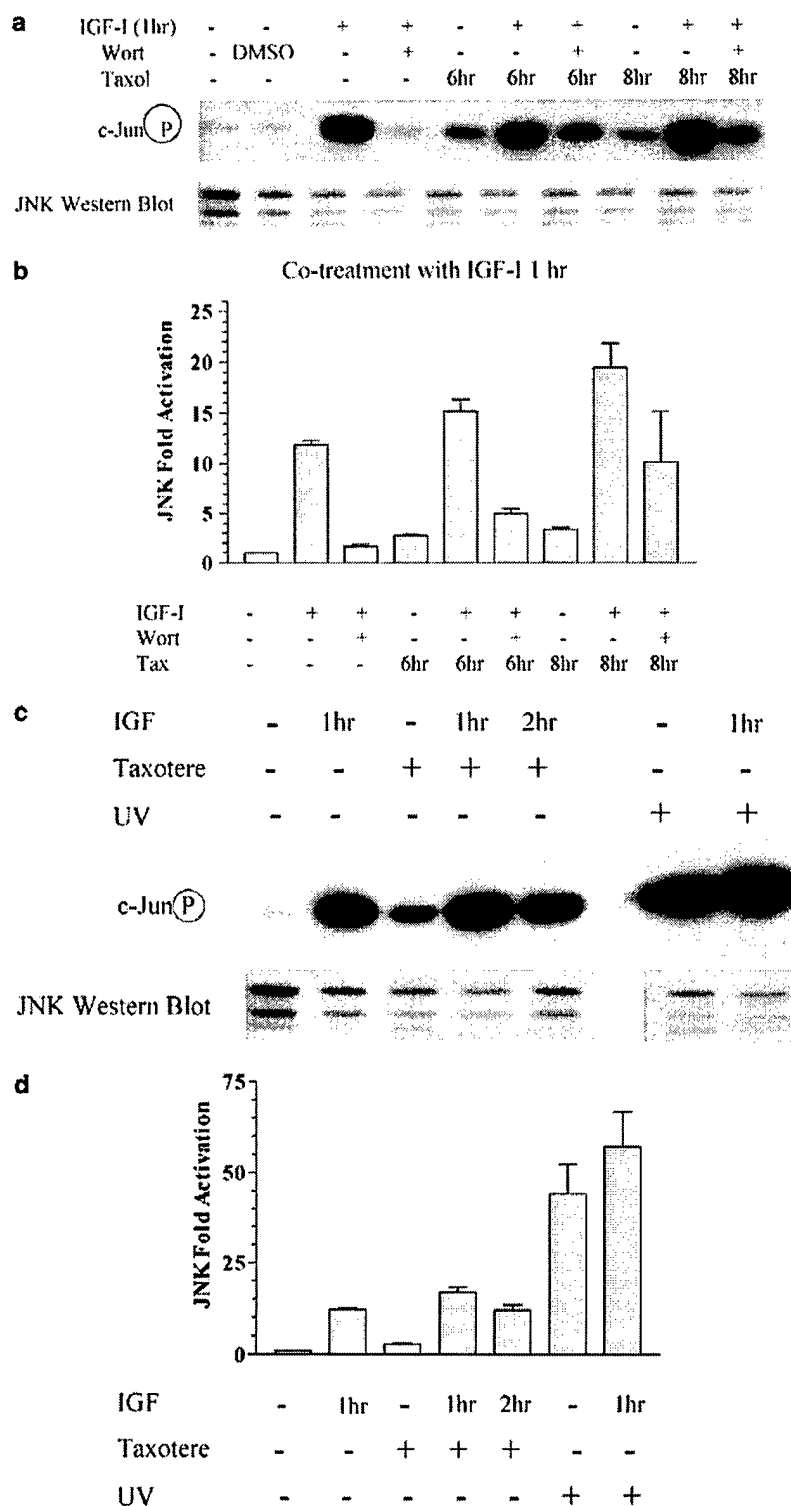
Figure 4 IGF-I and chemotherapy cotreatment results in additive effects on JNK. (a) JNK activity was measured by exposing MCF-7 cells to Taxol (0.25 μM) and IGF-I (50 ng/ml). Cells were exposed to wortmannin (100 nM) for 40 min at concentrations indicated prior to IGF-I treatment. Western blot analyses of kinase reactions were performed to compare JNK protein levels for each treatment. (b) Graphical representation of the above kinase assays showing the combined results of at least two independent experiments (mean ± range). (c) The effect of IGF-I cotreatment with Taxotere (1 μM for 2 h) and UV (50 J/M² for 50 min) on JNK activity was tested by exposing cells to each treatment until time of maximal response of each treatment. Western blot analysis was performed to compare JNK expression in each treatment. (d) Each graph shown represents three independent experiments (mean ± s.e.m.)

that induce JNK activity like Taxotere and UV (Figure 4c and d). Western blots assessing total JNK protein in kinase reactions confirm that changes in JNK activity are not a result of changes in the amount of JNK protein in the various samples. Because of the large increase in JNK activity induced by UV, significant increases with IGF-I cotreatment were more difficult to observe. Since cotreatment with IGF-I and chemotherapy led to an increase in JNK activity, we sought to determine if this activation is reduced by PI 3-kinase inhibition. Wortmannin inhibited JNK activity in IGF-I treated samples (Figure 4a and b). These data show that both stress treatment and IGF-I treatment enhance JNK activity and indicate that IGF-I survival responses may be mediated in a complex manner involving both JNK and Akt activation. JNK activation by both stress and growth factor treatment may also indicate complex signaling through different isoforms, resulting in different biological responses (Potapova et al., 2000; Chen et al., 2001; She et al., 2002). Next, we set out to characterize the roles of IGF-I-activated JNK and Akt on cellular outcome(s).

Akt, but not JNK, enhances IGF-I cytoprotection

First, we needed to confirm that Akt is activated by IGF-I treatment in MCF-7 cells. We developed a kinase-specific substrate using the Akt consensus binding sequence of GSK (a well-characterized Akt substrate) to investigate the involvement of downstream Akt activity in PI 3-kinase-dependent survival in our model. In vitro kinase assays confirmed that IGF-I treatment of MCF-7 cells induced Akt maximally at 10 min of exposure (Figure 5a) and that pretreatment with the PI 3-kinase inhibitors, LY294002 (Figure 5b) or wortmannin (data not shown), reduced IGF-I induction of Akt. Increased Akt activity was observed both when Akt was isolated by immunoprecipitation (data not shown), and when Akt-containing cell lysates were exposed to an immobilized Akt-specific substrate,

GST-GSK, following IGF-I treatment. These results support that PI 3-kinase and Akt may elicit IGF-I survival effects in MCF-7 cells. In T47D cells, Akt is phosphorylated even in the absence of growth factor indicating that PI 3-kinase activity may be constitutive in that cell line (data not shown).

In order to more clearly decipher the potential role of either JNK or Akt in IGF-I cytoprotection, MCF-7 cells were stably transfected with either Wt Akt, Wt JNK, Mt Akt (K179A, kinase dead), or Mt JNK (T183A/Y185F, kinase dead) HA-tagged constructs. Stable transfectants were plated in chamber slides, serum-starved overnight, and treated cells were exposed to Taxol or IGF-I treatment alone or in combination. Figure 6a shows that IGF-I significantly reduced apoptosis induced by Taxol (test for overall effect, $P < 0.0001$). IGF-I reduced cell death in parental and Mt Akt-transfected cells by 59 and 53%, respectively, compared to Taxol treatment alone. Cells overexpressing Wt Akt experienced a 34% reduction in apoptosis with IGF-I treatment ($P = 0.056$). The lack of a significant effect of IGF-I on Wt Akt-expressing cells appears to be because of the dramatic effect that overexpression of Wt Akt has on Taxol's ability to induce apoptosis in these cells. Wt Akt overexpressing cells underwent 70% less apoptosis than parental MCF-7s treated with Taxol alone (13 versus 44%, $P < 0.0001$). We did not observe a significant difference between Mt Akt transfectants and parental cells with respect to IGF-I protection from Taxol-induced apoptosis. These latter results suggest either that another IGF-I-dependent pathway may counteract Mt Akt effects or that Mt Akt overexpression was not able to squelch endogenous Akt signaling in response to IGF-I.

Cells transfected with Wt or Mt JNK were treated in a similar fashion as described above (Figure 6b). Overall, parental control groups were very similar to those in Akt experiments; in JNK experiments, IGF-I reduced Taxol-induced apoptosis in parental cells by 60 versus 59% in Akt experiments (Figure 6a and b). Comparison

a

Akt Fold Induction (y-axis, 0.0 to 4.5)
IGF-I Exposure (minutes) (x-axis, 0 to 30)

b

GSK (P)

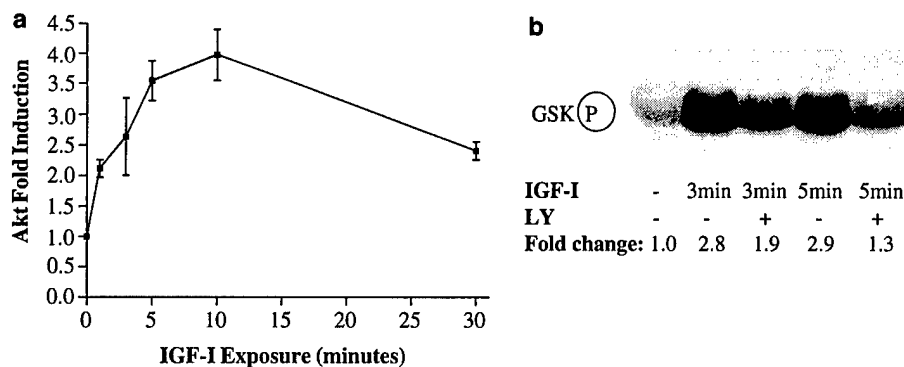| IGF-I	-	3min	3min	5min	5min
LY	-	-	+	-	+
Fold change:	1.0	2.8	1.9	2.9	1.3

Figure 5 GST-Akt peptide substrate is phosphorylated by IGF-I-treated MCF-7 cell lysates. GST-Akt-specific substrate (GST-GSK) was developed as described in Materials and methods. (a) MCF-7 cells were treated with IGF-I 50 ng/ml and at the indicated times as described in Materials and methods. Phosphorylated GST-GSK product resulting from in vitro kinase assays was detected and measured. The graph shown represents three independent experiments (mean ± s.e.m.). (b) MCF-7 cells were either preincubated in 50 μM LY294002 (LY) for 40 min prior to IGF-I treatment or treated with IGF-I alone, as indicated. Phosphorylated GST-GSK was analysed using SDS–PAGE and autoradiography
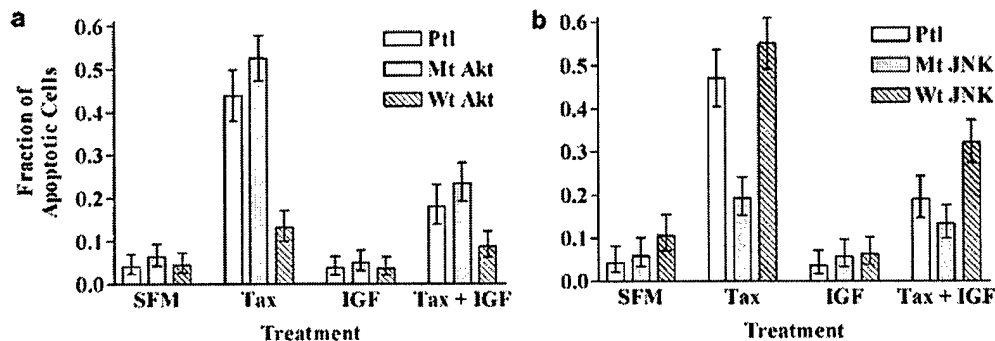
Figure 6 Overexpression of Mt Akt or Wt JNK enhanced Taxol-induced apoptosis and reduced IGF-I survival effects. (a) Parental (Ptl) MCF-7 cells and wildtype (Wt) or mutant (Mt) Akt MCF-7 transfectants were plated in chamber slides and treated as described in Materials and methods. Cells were stained with Hoechst 33258 for analysis of apoptotic nuclei 48 h after exposure. (b) Parental MCF-7 cells and Wt or Mt JNK MCF-7 transfectants were tested in the same fashion as Akt transfectants above. Bars are the average of three independent experiments for both Akt and JNK experiments. Error bars show 95% CI around the mean
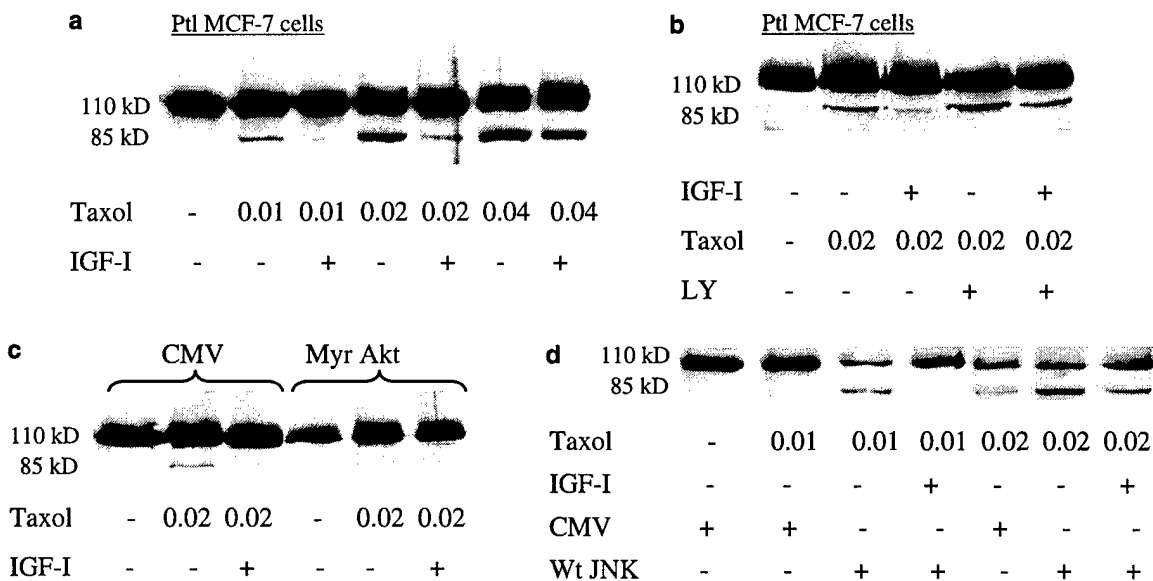

Figure 7 IGF-I inhibits Taxol-mediated apoptosis while Wt JNK overexpression enhances PARP cleavage induced by Taxol. In each experiment, parental and transfected MCF-7 cells were serum-starved overnight. Taxol treatment was added at increasing concentrations (0.01–0.04 μM, as indicated) with or without IGF-I cotreatment (50 ng/ml), as indicated. At 48 h after treatment, cells were lysed and PARP cleavage was measured by Western blot analysis of parental and cleaved PARP fragments. The presence of an 85 kDa cleavage fragment indicates induction of apoptosis. (a) IGF-I inhibited PARP cleavage at Taxol concentrations less than 0.04 μM/ml. (b) Cells were treated in the same fashion as above but some cells were cotreated with or without IGF-I and LY294002 (50 μM) for 40 min as indicated. (c) Transient transfection of MCF-7 cells using empty vector and a Myr Akt-containing plasmid was performed and then cells were treated as described above. (d) MCF-7 cells and stable Wt JNK transfectant cells were treated in the same fashion described above. PARP cleavage was analysed by Western blot using a PARP primary antibody

of all treatment groups of Wt JNK transfectants to parental cells demonstrates that overexpression of Wt JNK results in a significant increase in apoptosis (test for overall effect, $P = 0.0001$). Figure 6b also shows that, similar to the effects of Wt Akt, transfection of cells with Mt JNK leads to a dramatic decrease in cell sensitivity to Taxol compared to parental cells, 19 versus 47% apoptosis ($P = 0.0009$). This lends further support to the hypothesis that JNK activity is transducing a cell death signal under cellular stress. Similar to the Wt Akt-transfected cells, we did not observe significant increases

in protection with Mt JNK overexpression when cells were cotreated with IGF-I.

Since the Hoechst apoptosis assay may be somewhat subjective, significant results were confirmed using PARP cleavage analysis using separate stable transfectant lines, shown in Figure 7. Using this assay, parental MCF-7 cells underwent apoptosis, as indicated by the appearance of a PARP cleavage fragment at 85 kDa, when treated with Taxol. Again, IGF-I protected from Taxol-induced PARP cleavage at Taxol concentrations up to 0.04 μM (Figure 7a). To clarify the role of Akt in

our model, we inhibited PI 3-kinase using LY294002, and we also determined the contribution of activated Akt in a fashion that eliminates other IGF-I- and PI 3-kinase-dependent pathways by using the myristylated form of Akt (myr-Akt) in transient transfections. Preincubation of MCF-7 cells with LY294002 enhanced Taxol-mediated PARP cleavage and inhibited IGF-I protection of cells (Figure 7b), while overexpression of myr-Akt blocked Taxol-induced apoptosis (Figure 7c), confirming that Akt mediates cell survival in Taxol-treated cells. However, data including the LY294002 compound must be interpreted with caution since this agent also inhibits JNK in our model. In contrast to these Akt data, overexpression of Wt JNK alone enhanced Taxol-induced PARP cleavage (Figure 7d). Further, using the Wt JNK transfectants we were still unable to demonstrate that JNK activation by IGF-I had any effect on cell survival. These observations may be explained either by the lack of a role for JNK in conveying an IGF-I survival responses or by a dominant effect of Taxol-induced JNK. The last possibility, which we were unable to ascertain in these studies, is the presence of JNK isoform responses that may be treatment dependent.

JNK inhibits MCF-7 AIG

We have previously established that IGF-I treatment of MCF-7 cells enhances AIG (Van Den Berg *et al.*, 1997). In order to determine if IGF-I induction of JNK results in a change in IGF-I-mediated responses in the absence of a strong stress treatment, we assessed the effect of JNK overexpression on IGF-I-enhanced colony formation (Figure 8). Stable transfectants of Wt and Mt JNK were compared to parental MCF-7 cells. Wt JNK overexpression alone strongly inhibited MCF-7 colony formation (comparing parental MCF-7 cells to Wt JNK transfectants), and it also blocked IGF-I enhancement of colony formation (comparing Wt JNK transfectants to Wt JNK transfectants + IGF-I), suggesting that JNK activation by IGF-I antagonizes IGF-I tumorigenic effects. Both Mt JNK transfectant samples, cultured in 5% CSS and 5% CSS + IGF-I treatment,

formed increased numbers of colonies that were similar to the parental MCF-7, IGF-I-treated controls. These data support the conclusion that IGF-I induction of JNK is inhibiting IGF-I proliferative or survival effects in MCF-7 cells.

Phosphorylation of IRS-1 human Ser^{312} is PI 3-kinase-dependent and increased in Wt JNK transfectants

Given our evidence that JNK inhibits IGF-I responses and that of other investigators showing that JNK can bind to IRS-1 and serine phosphorylate rat Ser^{307} (human Ser^{312}), we decided to determine if this response could be a potential mechanism for the observed inhibitory effect of JNK by IGF-I treatment in our cells. Parental MCF-7 cells were pretreated with LY294002 in some instances prior to treating the cells with IGF-I or Taxol. Total IRS-1 was immunoprecipitated, and isolated protein was analysed using a rat IRS-1 antibody Ser^{307} (corresponding to human Ser^{312}) for Western blot analysis. Figure 9a shows that IGF-I treatment of parental MCF-7 cells enhances phosphorylation of Ser^{312} at times where peak JNK activation by IGF-I was observed in these cells. Further, this activity was blocked by inhibiting PI 3-kinase with LY294002. Taxol treatment also increased Ser^{312} phosphorylation (Figure 9b), indicating that JNK may be mediating phosphorylation of this serine site. In Figure 9c, cells were transfected using either empty vector or a GST-Wt JNK containing plasmid. After serum starvation, transfected cells were treated with IGF-I and LY294002 as described above. IRS-1 was immunoprecipitated from cleared cell lysates using a total IRS-1 antibody. Western blot analysis was performed using the rat Ser^{307} IRS-1 antibody. Again, IGF-I treatment of cells enhanced Ser^{312} (rat Ser^{307}) phosphorylation and LY294002 pretreatment inhibited IGF-I-dependent serine phosphorylation. In these experiments, an increase in IGF-I-mediated serine phosphorylation was observed in the Wt JNK transfectants compared to mocked transfected cells. Further, pretreatment with LY294002 inhibited serine phosphorylation in both mock and Wt JNK-transfected cells, supporting the conclusion that
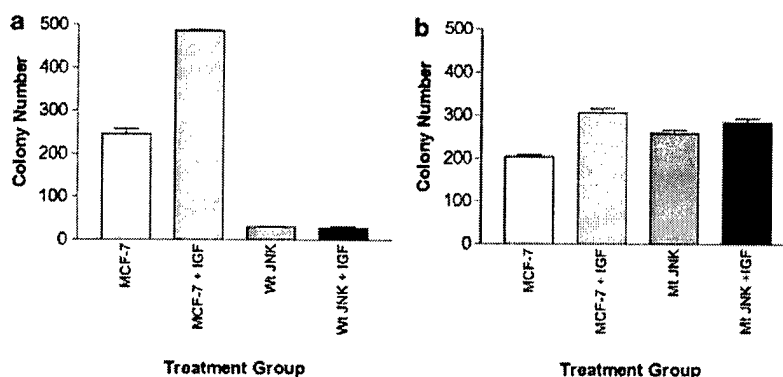

Figure 8 JNK overexpression inhibits AIG and IGF-I stimulated AIG. Parental MCF-7 cells and stable Wt and Mt JNK transfectant MCF-7 cells were suspended in 5% CSS and 0.8% Seaplaque agarose. Cells were seeded at 30 000 per dish and grown for 9 days. IGF-I (50 ng/ml) was added as indicated. Each sample was grown in triplicate and colonies were counted within the same surface area
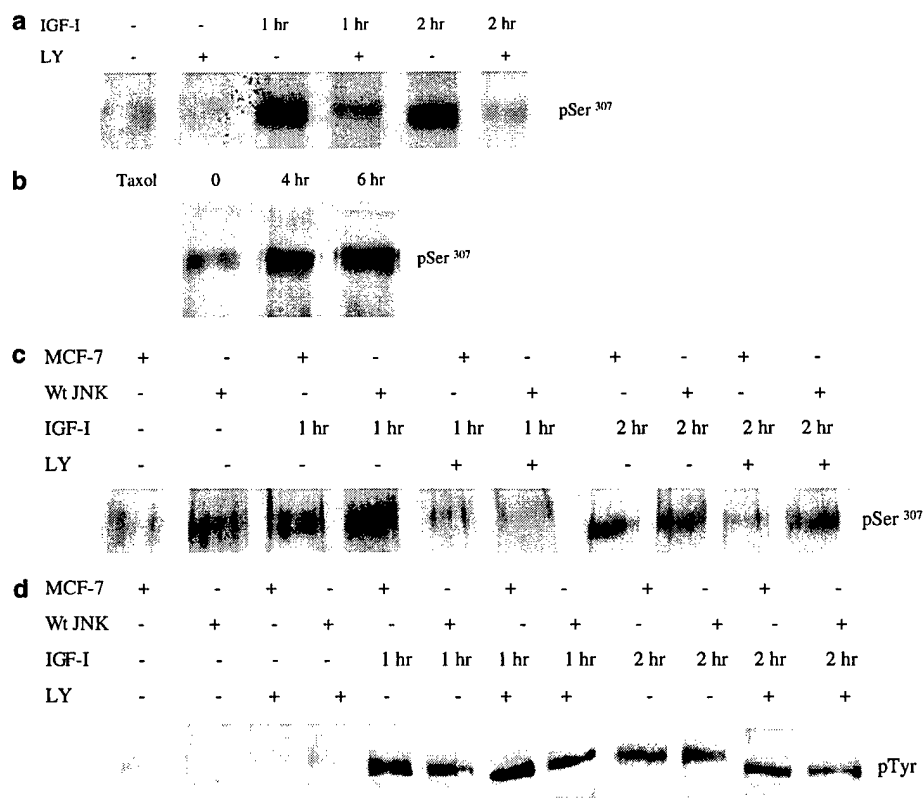
Figure 9 IGF-I and Taxol treatments lead to Ser^{312} phosphorylation of IRS-1 and IGF-I effects were blocked by PI 3-kinase inhibition. MCF-7 cells were plated overnight, then serum-starved. Some samples were pretreated with LY294002 100 μM for 40 min, as indicated. Cells were treated with IGF-I (50 ng/ml) or Taxol (0.25 μM) for the duration of the time indicated. All cells were lysed at the indicated times, lysates were cleared, and IRS-1 was immunoprecipitated using a total IRS-1 antibody. Ser^{312} phosphorylation was measured using a rat Ser^{307}-specific antibody, which specifically cross-reacts with human phosphoserine 312. (a) Phosphorylation of IRS-1 Ser^{312} in IGF-I-treated cells and the effect of PI 3-kinase inhibition with LY294001 was assessed by Western blot analysis. (b) Phosphorylation of IRS-1 Ser^{312} in Taxol (0.25 μM)-treated MCF-7 cells was assessed using methods described above. (c) MCF-7 cells were transiently transfected as described in Materials and methods. Ser^{312} phosphorylation of mock-transfected cells was compared to Wt JNK transfectants. (d) Tyrosine phosphorylation of IRS-1 was measured in parental MCF-7 cells and Wt JNK transfectants using an antiphosphotyrosine specific antibody for Western blot analysis

IGF-I-mediated phosphorylation of Ser^{312} is PI 3-kinase dependent. Further, we assessed the potential role of JNK activity on tyrosine phosphorylation of IRS-1. Immunoprecipitates of total IRS-1 were analysed for tyrosine phosphorylation by Western blot analysis using an antiphosphotyrosine antibody. Tyrosine phosphorylation of IRS-1 was robust after 1 h and somewhat less at 2 h of IGF-I treatment. Cotreatment with the LY294002 did not appear to inhibit tyrosine phosphorylation, but these samples of IRS-1 migrated more rapidly, possibly indicating less serine phosphorylation. Interpretation of IRS-1 tyrosine phosphorylation data using the LY294002 inhibitor is complex, given that it also inhibits Akt. Akt phosphorylates IRS-1 at sites not including Ser^{312} however, this serine phosphorylation activity is thought to prevent tyrosine dephosphorylation of IRS-1 (Paz et al., 1999). Finally, Wt JNK transfectant cells had slightly less tyrosine phosphorylation compared to MCF-7 cells. With these considerations in mind, our data support the conclusion that IGF-I-activated JNK

may result in serine phosphorylation of IRS-1, but it is unclear if this action results in an inhibitory tyrosine phosphorylation effect on IRS-1 and its ability to mediate IGF-I signaling in breast cancer cells.

Discussion

In this paper, we demonstrate that IGF-I has potent effects on JNK and Akt activity. IGF-I activation of both PI 3-kinase and Akt supports the hypothesis that this pathway is essential for IGF-I-mediated chemoprotection. These data, along with apoptosis experiments using Wt and Mt Akt transfectants, further confirm our previous results showing that pharmacologic inhibition of PI 3-kinase and its downstream kinases enhanced both doxorubicin- and Taxol-induced apoptosis (Gooch et al., 1999). Additionally, use of a myr-Akt construct confirmed that enhanced Akt activity has a strong cell survival effect.

The large degree of JNK activation by IGF-I was somewhat surprising since activation of other tyrosine kinase receptors does not typically induce JNK to the same level or time to maximal stimulation as we observed (Kyriakas *et al.*, 1994; Westwick *et al.*, 1994; Fanger *et al.*, 1997; Goedert *et al.*, 1997; Alblas *et al.*, 1998). For example, other investigators (Miller *et al.*, 1996; Desbois-Mouthon *et al.*, 1998) have reported that insulin treatment of CHO or Rat 1 HIR fibroblasts activates JNK within 10–15 min of exposure. This activity results in an increase in AP-1 DNA binding and possibly cell proliferation (Miller *et al.*, 1996). Given that IGF-I induction of JNK is notably higher than what has been reported with other growth factors and since other growth factors induce proliferation through JNK (Bost *et al.*, 1997), we were initially perplexed by our results showing a lack of IGF-I proliferative (data not shown) or survival responses through JNK.

Activated PI 3-kinase has previously been shown to be upstream of JNK after exposure to other growth factors like platelet-derived growth factor (PDGF), and in some cases EGF, but not after exposure to UV irradiation or osmotic shock (Logan *et al.*, 1997; Lopez-Ilasaca *et al.*, 1997). Other investigators report that despite IGF-I's limited ability to induce JNK in embryonic kidney 293 cells, pretreatment with IGF-I suppresses JNK stimulation by TNFα and anisomycin (Okubo *et al.*, 1998). These investigators stressed the necessity of IGF-I pretreatment in order to observe inhibition of JNK in response to cellular stress; however, we did not study the effects of IGF-I pretreatment in our model. Also, these investigators did not study JNK response to IGF-I treatment alone beyond 1 h of exposure. In our model, we observed maximal activity after 2 h of IGF-I exposure. Given these mixed results reported by others, we initially anticipated that if IGF-I had any measurable effect on JNK it might be to abrogate chemotherapy induction of JNK. It is now clear that although chemotherapy drugs activate JNK, IGF-I induced JNK to a far greater extent in our breast cancer model. Cotreatment with chemotherapy and IGF-I further enhanced JNK activity, despite their opposing effects on cell survival.

The biological effect of overexpressed JNK suggests that even though it was induced both by Taxol and IGF-I, JNK's primary effect appears to be proapoptotic rather than protective. More so, IGF-I lost its cytoprotective effect in cells overexpressing JNK, where the stoichiometry of JNK versus Akt protein levels may have allowed JNK-induced apoptotic response to overcome some of the IGF-I-mediated Akt effects in these cells. Further, we show that JNK activity inhibited IGF-I responses, in the absence of stress, by reducing colony formation in the AIG assay and inhibiting the IGF-I-mediated increase in colony growth. Thus, we turned our attention to potential mechanisms of inhibition of IGF-IR signaling.

Much attention has recently been drawn to IRS phosphorylation of serine residues that may result in feedback inhibition of IR and IGF-IR downstream signaling or insulin resistance in diabetic models. Predictors of such biological responses focus on both the inhibition of IRS tyrosine-phosphorylation and the ability of serine-phosphorylated IRS proteins to bind and become phosphorylated by IR. Ser[307] of IRS-1 has become particularly interesting since it lies adjacent to the protein tyrosine binding (PTB) domain, the region required for receptor binding (Aguirre *et al.*, 2002). In diabetic models, JNK (activated by TNFα-, anisomysin-, and PI 3-kinase-sensitive kinases) phosphorylates this site to inhibit IRS downstream signaling (Rui *et al.*, 2001). In contrast, the PI 3-kinase-sensitive kinase, Akt, has four consensus serine phosphorylation motifs in IRS-1, not including Ser[307], which when phosphorylated inhibits tyrosine dephosphorylation of IRS-1 resulting in prolonged IRS-1-mediated responses (Paz *et al.*, 1999). The region containing Ser[307] also does not appear to be a phosphorylation motif for other kinases reported to phosphorylate IRS-1, including MAPK and PI 3-kinase (De Fea and Roth, 1997). Further, the stress kinase p38 is an unlikely candidate in our model since IGF-I treatment does not enhance its activity in MCF-7 cells (data not shown). Interestingly, Rui *et al.* (2001) have predicted that kinases other than just JNK may phosphorylate rat IRS-1 Ser[307]. This conclusion was based on data showing TNFα stimulation of Ser[307] phosphorylation is inhibited by PD98059. Although LY294002 blocked serine phosphorylation, it did not inhibit insulin activation of JNK after a 10 min exposure time. It is unclear if JNK may be activated at later time points in this model. However, since LY294002 cotreatment completely inhibited JNK activation by IGF-I and since IGF-I-mediated Ser[312] phosphorylation in our cells is also mediated by a PI 3-kinase-sensitive kinase, JNK is the most likely sole mediator of this effect. Further, Taxol treatment both activated JNK and enhanced human Ser[312] phosphorylation of IRS-1 in our model.

To our knowledge, little is published regarding the subsequent biological effects of growth factor activation of JNK in diabetic or cancer models, particularly looking at the combined effects of growth factors and chemotherapeutic agents in cancer models. These responses may be particularly relevant given that many solid tumors, including breast, prostate, lung, and colon cancer, commonly overexpress IGF-IR. These tumors are also often treated with chemotherapeutic agents. Intuitively, one may anticipate that the serine phosphorylation of downregulatory sites such as Ser[312] of IRS-1 and subsequent tyrosine dephosphorylation may be observed to a much lesser degree in cancer cells compared to normal cells. Our results indicate that phosphorylation of Ser[312] is quite high in cancer cells. On the other hand, we did not observe a very significant decrease in IRS-1 tyrosine-phosphorylation using JNK overexpression approaches. Inhibition of PI 3-kinase in MCF-7 cells and JNK transfectants resulted in faster mobility of tyrosine-phosphorylated IRS-1 indicating a reduction in serine phosphorylation. These data lead to uncertainty as to whether serine phosphorylation of IRS-1 actually inhibits its ability to serve as an IGF-IR substrate in breast cancer cells. We have not yet studied
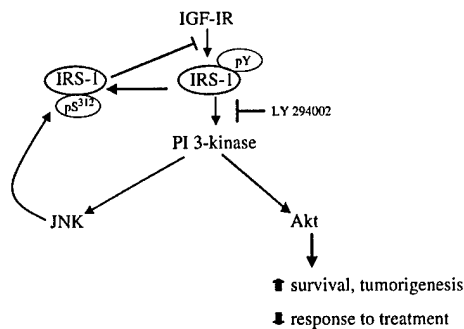
Figure 10 IGF-I activates JNK, which then inhibits IGF-IR-mediated signaling by serine phosphorylation of IRS-1. Our data support the proposed model where IGF-I activation of JNK leads to a negative feedback effect on IGF-IR signaling. This effect is observed when JNK is activated downstream of PI 3-kinase, and subsequently, activated JNK phosphorylates Ser^{312} of IRS-1 to inhibit IGF-IR responses

this interaction in our model. Somewhat in contrast to our model, Hemi *et al.* (2002) report that IRS-1 serine phosphorylation was enhanced by anisomycin, TNFα, and Smase (sphingomyelinse) treatment via phosphorylation of ErbB2 and 3 in Fao hepatoma cells, but that tyrosine phosphorylation of IRS-1 was inhibited by LY294002. Interestingly, JNK activity in response to the above treatments was not assessed in this paper but there data may implicate the complexity of PI 3-kinase signaling through both Akt and JNK (Figure 10). These findings also underline the relevance of crosstalk among stress- and growth factor-related pathways that may

converge on JNK and may be directly applied to cancer models as a therapeutic target.

Clearly, the biological role(s) of JNK are controversial (see review by Minden and Karin, 1997). Simple activation of JNK by any agonist does not imply the same biological response. JNK activity may either convey resistance or sensitivity to cellular stress (Fuchs *et al.*, 1998; Okubo *et al.*, 1998) or even proliferative responses (Bost *et al.*, 1997). Some investigators have begun to study the effects of diverse stimuli on kinases upstream of JNK and differential regulation resulting from the various JNK isoforms derived from the three JNK genes, JNK1, JNK2, and JNK3 (Gupta *et al.*, 1996; Cuenda *et al.*, 1997) in attempts to understand the various biological responses associated with JNK activity. Our findings that IGF-I and stress treatments activate JNK to inhibit IGF-I signaling make JNK an excellent target for cancer treatment. Inducing JNK response may simultaneously enhance the efficacy of radio- and chemotherapy as well as attenuating IGF-IR responses in cancer models.

References

Aguirre V, Werner ED, Giraud J, Lee YH, Schoelson SE and White MF. (2002). *J. Biol. Chem.*, **277**, 1531–1537.

Alblas J, Slager-Davidov R, Steenbergh PH, Sussenbach JS and van der Burg B. (1998). *Oncogene*, **16**, 131–139.

Bost F, McKay R, Dean N and Mercola D. (1997). *J. Biol. Chem.*, **272**, 33422–33429.

Brunet A, Bonni A, Zigmond MJ, Lin MZ, Juo P, Hu LS, Anderson MJ, Arden KC, Blenis J and Greenberg ME. (1999). *Cell*, **96**, 857–868.

Butler AA, Blakesley VA, Tsokos M, Pouliki V, Wood TL and LeRoith D. (1998). *Cancer Res.*, **58**, 3021–3027.

Cardone MH, Roy N, Stennicke HR, Salvesen GS, Franke TF, Stanbridge E, Frisch S and Reed JC. (1998). *Science*, **282**, 1318–1321.

Chen Y-R, Meyer CF and Tna T-H. (1996). *J. Biol. Chem.*, **271**, 631–634.

Chen N, Nomura M, She QB, Ma WY, Bode AM, Wang L, Flavell RA and Dong Z. (2001). *Cancer Res.*, **61**, 3908–3912.

Cuenda A, Cohen P, Buee-Scherrer V and Goedert M. (1997). *EMBO J.*, **16**, 295–305.

Cullen KJ, Yee D, Sly WS, Perdue J, Hampton B, Lippman ME and Rosen N. (1990). *Cancer Res.*, **50**, 48–53.

Datta SR, Dudek H, Tao X, Masters S, Fu H, Gotoh Y and Greenberg ME. (1997). *Cell*, **91**, 231–241.

De Fea K and Roth RA. (1997). *J. Biol. Chem.*, **272**, 31400–31406.

Desbois-Mouthon C, Blivet-Van Eggelpoel M-J, Auclair M, Cherqui G, Capeau J and Caron M. (1998). *Biochem. Biophys. Res. Commun.*, **243**, 765–770.

Dunn SE, Ehrlich M, Sharp NJH, Solomon G, Hawkins R, Baserga R and Barrett JC. (1998). *Cancer Res.*, **58**, 3353–3361.

Fanger GR, Lassignal Johnson N and Johnson GL. (1997). *EMBO J.*, **16**, 4961–4972.

Franke TF, Yang S-I, Chan TO, Datta K, Kaziauskas A, Morrison DK, Kaplan DR and Tsichlis PN. (1995). *Cell*, **81**, 727–736.

Fuchs SY, Fried VA and Ronai Z. (1998). *Oncogene*, **17**, 1483–1490.

Goedert M, Cuenda A, Craxton M, Jakes R and Cohen P. (1997). *EMBO J.*, **16**, 3563–3571.

Gooch JL, Van Den Berg CL and Yee D. (1999). *Breast Cancer Res. Treatment*, **56**, 1–10.

Gupta S, Barrett T, Whitmarsh AJ, Cavanagh J, Sluss HK, Derijard B and Davis RJ. (1996). *EMBO J.*, **15**, 2760–2770.

Hemi R, Paz K, Wertheim N, Karasik A, Zick Y and Kanety H. (2002). *J. Biol. Chem.*, **277**, 8961–8969.

Hermanto U, Zong CS and Wang LH. (2000). *Cell Growth Differ.*, **12**, 655–664.

Hibi M, Lin A, Smeal T, Minden A and Karin M. (1993). *Genes Dev.*, **7**, 2135–2148.

Kennedy SG, Wagner AJ, Conzen SD, Jordan J, Bellacosa A, Tsichlis PN and Hay N. (1997). *Genes Dev.*, **11**, 701–713.

Kyriakas JM, Banerjee P, Nikolakaki E, Dai T, Rubie EA, Ahmad MF, Avruch J and Woodget JR. (1994). *Nature (London)*, **369**, 156–159.

Lee AV, Gooch JL, Oesterrich S, Guler RL and Yee D. (2000). *Mol. Cell. Biol.*, **20**, 1489–1496.

Logan SK, Falasca M, Hu P and Schlessinger J. (1997). *Mol. Cell. Biol.*, **17**, 5784–5790

Lopez-Ilasaca M, Li W, Uren A, Yu J, Kazlauskas A, Gutkind JS and Heideran MA. (1997). *Biochem. Biophys. Res. Commun.*, **232**, 273–277.

Miller BS, Shankavaram UT, Horney MJ, Gore ACS, Kurtz DT and Rosenzweig SA. (1996). *Biochemistry*, **35**, 8769–8775.

Minden A and Karin M. (1997). *Biochim. Biophys. Acta*, **1333**, F85–F104.

Mitsuuchi Y, Johnson SW, Selvakumaran M, Williams SJ, Hamilton TC and Testa JR. (2000). *Cancer Res.*, **60**, 5390–5394.

Monno S, Newman MV, Cook M and Lowe W. (2000). *Endocrinology*, **141**, 544–550.

Okubo Y, Blakesley VA, Stannard B, Gutkind S and Le Roith D. (1998). *J. Biol. Chem.*, **273**, 25961–25966.

Paz K, Liu Y-F, Shorer H, Hemi R, LeRoith D, Quan M, Kanety H, Seger R and Zick Y. (1999). *J. Biol. Chem.*, **274**, 28816–28822.

Peyrat JP, Bonneterre J, Jammes H, Beuscart R, Hecquet B, Djiane J, Lefebvre J and Demaille A. (1990). *J. Steroid Biochem. Mol. Biol*, **37**, 823–827.

Potapova O, Gorospe M, Dougherty RH, Dean NM, Gaarde WA and Holbrook NJ. (2000). *Mol. Cell. Biol.*, **20**, 1713–1722.

Potapova O, Haghighi A, Bost F, Liu C, Birrer MJ, Gjerset R and Mercolas D. (1995). *J. Biol. Chem.*, **272**, 14041–14044.

Resnik JL, Reichart DB, Huey K, Webster NJG and Seely BL. (1998). *Cancer Res.*, **58**, 1159–1164.

Rosette C and Karin M. (1996). *Science*, **274**, 1194–1197.

Rui L, Aguirre V, Kim JK, Shulman GI, Lee A, Corbould A, Dunaif A and White MF. (2001). *The Journal of Clinical Investigation* **107**, 181–189.

She QB, Chen N, Bode AM, Flavell RA and Dong Z. (2002). *Cancer Res.*, **62**, 1343–1348.

Singer C, Rasmussen A, Smith HS, Lippman ME, Lynch HT and Cullen KJ. (1995). *Cancer Res.*, **55**, 2448–2454.

Sluss, H.K., Barrett, T., Derijard, B. and Davis, R.J. (1994). *Mol Cell. Biol.*, **14**, 8376–8384.

Smith DB and Johnson KS. (1988). *Gene*, **67**, 31–40.

Van Den Berg CL, Cox GN, Stroh CA, Hilsenbeck SG, Weng C, McDermott MJ, Pratt D and Yee D. (1997). *Eur. J. Cancer*, **33**, 1108–1113.

Wang T-H, Eang H-S, Ichijo H, Giannakakou P, Foster JS, Fojo T and Wimalasena J. (1998). *J. Biol. Chem.*, **273**, 4928–3936.

Westwick JK, Weitzel C, Minden A, Karin M and Brenner DA. (1994). *J. Biol. Chem.* 26396–26401.

Whitmarsh AJ, Shore P, Sahrrocks AD and Davis RJ. (1995). *Science*, **269**, 403–407.